

How Much Stress Is Implied by Dodd-Frank Annual Stress Test (DFAST) Scenarios?

J. R. STOKES[†]

University of Northern Iowa

January 2016

Abstract Since the passage of the Dodd Frank Wall Street Reform and Consumer Protection Act, many financial institutions have been developing and validating stress testing models and methodologies. A key feature of the Act is the Dodd Frank Annual Stress Test (DFAST) consisting of regulator prescribed stress scenarios. However, little is known about the extent of the stress implied by the scenarios beyond their ordinal descriptions as baseline, severe, and severely adverse. In this paper, Kullback-Leibler divergence is suggested as a mechanism to assess how much stress is implied by each scenario. In general, the results suggest that the adverse scenario is a reasonably stressful scenario while the severely adverse scenario may be consistent with such an unprecedented level of stress that it may actually undermine its usefulness as a plausible scenario for stress testing. An example is also provided showing how the methods developed can be applied to assist in the identification of plausible and consistent stress for non-DFAST variables.

Keywords: Dodd-Frank, DFAST, entropy, Kullback-Leibler divergence, stress testing

JEL Classification: G02, Q18, G21, C14, C58

[†] 313 Curris Business Building, Cedar Falls, IA 50614-0124. Email: jeffrey.stokes@uni.edu. Any errors or omissions are the sole responsibility of the author,

1 Introduction

With the passage of the Dodd Frank Wall Street Reform and Consumer Protection Act (hereafter Act or Dodd-Frank) many financial companies have been developing and validating stress testing models and methodologies. A key feature of the Act is detailed in Section 165(i) which requires nonbank financial companies supervised by the Board of Governors (BOG) and bank holding companies to conduct semiannual stress tests (hereafter Dodd-Frank stress test or DFAST) and all other financial companies with total consolidated assets of \$10 billion or more to conduct annual stress tests. The stress tests are designed to determine whether these companies have the capital necessary to absorb losses as a result of adverse economic conditions. Capital has been shown by Berger and Bouwman (2013) to increase all banks' performance during banking crises and additionally small bank performance during market crises as well as normal times. Stress test results must be reported to the BOG and to the company's primary financial regulatory agency¹.

According to the specifics of DFAST, the BOG must provide at least three different sets of conditions or scenarios under which the stress tests are to be conducted. The most recent release of baseline, adverse, and severely adverse DFAST scenarios consist of 16 macroeconomic variables describing economic developments within the United States and essentially 12 macroeconomic variables (three variables in four countries or country blocks) describing international economic conditions spanning the 13 quarters from Q3 2014 to Q4 2017². The scenarios are not meant to be interpreted as BOG predictions but rather hypothetical scenarios that, as noted above, are designed to be used to assess the financial strength of companies and their resilience to adverse economic environments. Financial companies would typically build their stress testing models around these or related economic variables that more closely influence their businesses.

Balasubramnian and Cyree (2014) conclude there is evidence that suggests market discipline on banking firms appears to have improved of late. Even so, several important risk management questions face financial companies especially in light of the DFAST portion of the Act. Perhaps first among them is the question of which macroeconomic variables should be used when conducting stress testing? Financial companies are free to use whatever macroeconomic variables make the most sense for their businesses. For example, a financial company with only a domestic footprint would likely only consider the domestic macroeconomic variables and more

¹ The relevant regulatory agencies are the Board of Governors of the Federal Reserve System, Office of the Comptroller of the Currency, and the Federal Deposit Insurance Corporation.

² The scenarios are discussed in detail in "2015 Supervisory Scenarios for Annual Stress Tests Required under the Dodd-Frank Stress Testing Rules and the Capital Plan Rule" Board of Governors of the Federal Reserve System, 2014 and in Section 4 of this paper.

likely a subset of these variables. In addition, some companies may find that macroeconomic variables that are not a part of the BOG's set of variables may make more sense for their businesses. Smaller regional companies, for example, may find that the nationally oriented macroeconomic variables are less useful for stress testing their portfolios. In such cases, the question of which economic variables to use, and how much stress to apply to emulate the BOG's adverse and severely adverse scenarios, becomes much more challenging.

A related question that is perhaps more fundamental has less to do with which are the most important macroeconomic variables for a company to choose and more to do with how much stress is implied by the scenarios in the first place. This is an especially important question for many financial companies in the \$10 billion to \$50 billion asset range in that these institutions are less likely to have the personnel on site with the technical expertise to develop stress testing models internally. Data are also likely an issue and it could be the case that more simple approaches to stress testing are warranted as a precursor to developing more complex stress testing models. For example, it is possible that a \$10 billion financial company with a small regional footprint should initially approach stress testing within a relatively simple Value-at-Risk (VaR) framework given their endowment of technical expertise and paucity of data. If so, the question of how much VaR stress to apply to be consistent with the BOG scenarios is critical to determine.

The central purpose of this paper is to report on an analysis of the severity of the DFAST stress testing scenarios set forth by the BOG. In section 2, some recent stress testing literature is reviewed and Kullback-Leibler (KL) divergence is discussed as one possible approach for measuring the amount of stress in the prescribed DFAST scenarios. The discussion is facilitated by exploiting a well-known linkage between primal and dual relative entropic models. Presented in Section 3 are two empirical examples using recently published data that help firm up the linkage between financial stress and the concept of KL divergence. In section 4, the main focus of the research is presented which is the estimation of the joint density for several of the BOG's macroeconomic variables and the subsequent quarterly measurement of KL divergence associated with each scenario. A simple example is also presented that shows how the models and methods developed here might be applied to generate a scenario path for a variable that is not one of the BOG variables, but is consistent with a given BOG scenario. Concluding remarks are presented in Section 5.

2 Plausible Stress and Kullback-Leibler Divergence

2.1 Stress Testing and Plausibility

While more recent tumult in the capital markets has garnered considerable attention with respect to the need for systematic approaches to stress testing, the idea is not new³. As examples, the Basel Accords and the concept of VaR both predate DFAST. Bangia *et al.* (2002) cite the turmoil in the capital markets in the late 1990s as a significant driver of the need for systematic stress testing of banks' portfolios. Since then, advances in the theory and application of stress testing methodologies have continued to develop. Recent examples include Abdymomunov and Gerlach (2014) who propose a new method for generating yield curve scenarios for stress tests, Alexander and Sheedy (2008) who propose a methodology for stress testing in the context of market risk models that can incorporate both volatility clustering and heavy tails, and Huang *et al.* (2009) who propose a framework for measuring and stress testing the systematic risk of a group of major financial institutions.

As noted by Abdymomunov and Gerlach (2014), stress testing scenarios are generally either historical or handpicked. Varotto (2012), for example, discusses the plausibility of the recent *Great Recession* as a historical scenario while Fender *et al.* (2001) reports that many banks use *Black Monday 1987* as a plausible historical scenario when stress testing equities. By contrast, an example of a handpicked scenario is presented in Miu and Ozdemir (2009) who develop a macrofactor stress testing model and apply the model to the oil and gas sector. The handpicked scenario chosen by Miu and Ozdemir (2009) is defined as a one standard deviation increase in the quarterly change in real GDP coupled with one standard deviation decreases in the annual change in global oil demand and the annual change in Scotiabank All Commodity Index. Obviously care must be taken to ensure that any handpicked scenarios are realistic and plausible.

Perhaps no one has advanced the theory of stress testing more than a series of papers that includes Breuer (2008), Breuer *et al.* (2009), Breuer and Csiszar (2010), Breuer *et al.* (2012), and Breuer and Csiszar (2013). In these papers, the authors develop models and methods for identifying plausible worst case scenarios for stress testing portfolios. These methods do not involve handpicked scenarios, but rather, are identified quantitatively using the concept of relative

³ See, for example, Fender *et al.* (2001) or the report from the *Committee on the Global Financial System* (2005) for analysis of survey data related to banks' use of stress testing models and scenarios.

entropy and the Maximum Loss Theorem (MLT)⁴. In the following section, the concept of relative entropy is discussed within the context of Information Theoretic (IT) econometric estimation and is then related directly to the dual of a model presented in Breuer and Csiszar (2013) (hereafter B&C) that is a direct result of the MLT.

2.1 Kullback-Leibler Divergence

Following Golan (2006), a (primal) generalized IT optimization problem in probability space can be expressed as

$$\begin{aligned} \bar{\mathbf{p}}^* &= \operatorname{argmin}\{D_{\delta+1}^R(\bar{\mathbf{p}} \parallel \mathbf{p})\} \\ \text{s.t.} \\ g_m(\mathbf{y}, \mathbf{x}, \bar{\mathbf{p}}) &= [\mathbf{0}], m = 1, 2, \dots, M \\ \bar{\mathbf{p}}'\mathbf{1} &= 1 \\ \bar{\mathbf{p}} &\geq 0 \end{aligned} \quad (1)$$

Here, $D_{\delta+1}^R(\bar{\mathbf{p}} \parallel \mathbf{p})$ is Rényi's (1961) measure of relative entropy between two discrete probability distributions $\bar{\mathbf{p}}$ and \mathbf{p} given δ . The constraints of the primal problem are a set of M zero moment consistency equations, $g_m(\cdot)$, parameterized by vectors of data, \mathbf{y} and \mathbf{x} , and the estimated probabilities, $\bar{\mathbf{p}}$, and constraints that ensure the probabilities are proper probabilities (i.e. sum to unity and non-negative). The model presented above is a generalization of models initially presented by Kitamura and Stutzer (1997) and Imbens *et al.* (1998).

Rényi's (1961) relative entropy is given by the function $D_{\delta+1}^R(\bar{\mathbf{p}} \parallel \mathbf{p}) = -\frac{1}{\alpha} \log[1 + \alpha(\alpha + 1)D_{\delta}^{CR}(\bar{\mathbf{p}} \parallel \mathbf{p})]$ where $D_{\delta}^{CR}(\bar{\mathbf{p}} \parallel \mathbf{p})$ denotes Cressie-Read (1984) relative entropy. As shown in Golan (2002), when $\delta \rightarrow 0$, $D_{\delta+1}^R(\bar{\mathbf{p}} \parallel \mathbf{p})$ reduces to Kullback-Leibler (KL) relative entropy or the KL divergent measure $D^{KL}(\bar{\mathbf{p}} \parallel \mathbf{p}) = \sum_i \bar{p}_i \ln\left(\frac{\bar{p}_i}{p_i}\right)$ ⁵. Under these conditions and assuming there are n possible states and a single moment consistency equation for data given by the vector \mathbf{l} , the primal generalized IT optimization problem (1) can be expressed as

$$\begin{aligned} \min D^{KL}(\bar{\mathbf{p}} \parallel \mathbf{p}) &= \bar{\mathbf{p}}' \ln\left(\frac{\bar{\mathbf{p}}}{\mathbf{p}}\right), \\ \text{s.t.} \\ \bar{\mathbf{p}}'\mathbf{l} &= \mathbb{E}(l), \\ \bar{\mathbf{p}}'\mathbf{1} &= 1 \\ \bar{\mathbf{p}} &\geq 0. \end{aligned} \quad (2)$$

⁴ Relative entropy is a broader concept than KL divergence although here, the two terms are used interchangeably.

⁵ In the IT econometric literature, KL divergence, as developed by Kullback and Leibler (1951), is often referred to as Shannon cross entropy in honor of Shannon (1948). As our interest here is in comparing the relative entropy or divergence between two probability distributions, we maintain the KL divergence descriptor.

If $l_i \in \mathbf{l}$ represents portfolio losses in the i th state, then $\mathbb{E}(l)$ is the total expected loss on the portfolio under a given worst case scenario. The vector of (worst case) probabilities to be estimated, $\bar{\mathbf{p}}$, are chosen relative to the reference distribution, \mathbf{p} , and $\mathbb{E}(l)$, both of which are exogenous in the model specification. The system presented in (2) is a primal representation of the dual optimization problem presented by B&C in their development of the MLT. To see this, consider that the Lagrangian equation for the primal constrained optimization IT problem given above in (2) is

$$\mathcal{L} = \sum_{i=1}^n \bar{p}_i \ln \left(\frac{\bar{p}_i}{p_i} \right) + \bar{\theta} \left(\mathbb{E}(l) - \sum_{i=1}^n \bar{p}_i l_i \right) + \bar{\mu} \left(1 - \sum_{i=1}^n \bar{p}_i \right) \quad (3)$$

where $\bar{\theta}$ and $\bar{\mu}$ are Lagrange multipliers. There are $n+2$ first order conditions (FOCs) given by the expressions: $1 + \ln \left(\frac{\bar{p}_i}{p_i} \right) - \bar{\theta} l_i - \bar{\mu} = 0, \forall i = 1, 2, \dots, n$, $\mathbb{E}(l) - \sum_{i=1}^n \bar{p}_i l_i = 0$, and $1 - \sum_{i=1}^n \bar{p}_i = 0$, the simultaneous solution of which results in the optimal minimizing values \bar{p}_i , $\bar{\theta}$, and $\bar{\mu}$.

Due to the nonlinearity of the FOCs, analytic solutions are not possible and the problem must be solved numerically. However, optimality implies that the stressed probabilities can be expressed as a function of the optimal multipliers as well as the reference probabilities, or

$$\bar{p}_i = p_i \exp(\bar{\theta} l_i + \bar{\mu} - 1) = \frac{p_i \exp(\bar{\theta} l_i)}{\sum_{j=1}^n p_j \exp(\bar{\theta} l_j)}. \quad (4)$$

These stressed or worst case probabilities are the same as those presented in B&C under the MLT⁶. Additionally, the denominator in (4) is known as a partition function in the entropy literature and is related to the function $\Lambda(\theta)$ from B&C, namely, $\sum_{j=1}^n p_j \exp(\bar{\theta} l_j) = \exp(\Lambda(\bar{\theta}))$.

The relationship between primal and dual optimization problems can be exploited to formally link the two approaches (see for example, Agmon *et al.*, 1979). Worst case scenario probabilities in (4) substituted into the KL divergence objective function in (2) yields

$$\bar{D}^{KL}(\bar{\mathbf{p}} \parallel \mathbf{p}) = \sum_i \left[\frac{p_i \exp(\bar{\theta} l_i)}{\exp(\Lambda(\bar{\theta}))} \right] \times \ln \left[\frac{\exp(\bar{\theta} l_i)}{\exp(\Lambda(\bar{\theta}))} \right]. \quad (5)$$

Rearranging terms, it follows that equation (5) can be rewritten as

⁶ See p. 1556 of Breuer and Csiszar (2013).

$$\begin{aligned}
\bar{D}^{KL}(\bar{\mathbf{p}} \parallel \mathbf{p}) &= \sum_i \left(\frac{p_i \exp(\bar{\theta} l_i)}{\exp(\Lambda(\bar{\theta}))} \right) \times [\bar{\theta} l_i - \Lambda(\bar{\theta})] \\
&= \bar{\theta} \sum_i \left(\frac{p_i l_i \exp(\bar{\theta} l_i)}{\exp(\Lambda(\bar{\theta}))} \right) - \Lambda(\bar{\theta}), \\
&= \bar{\theta} \Lambda'(\bar{\theta}) - \Lambda(\bar{\theta})
\end{aligned} \tag{6}$$

which is precisely: $\bar{D}^{KL}(\bar{\mathbf{p}} \parallel \mathbf{p}) = k$, the equation outlined by B&C in their application of the MLT.⁷ It is the numerical solution of this equation that yields $\theta = \bar{\theta}$ from which the stressed probabilities can be calculated. It is also clear that at $\theta = \bar{\theta}$, $\bar{D}^{KL}(\bar{\mathbf{p}} \parallel \mathbf{p}) = k$ and the plausibility parameter exogenous in B&C's model specification is precisely the KL divergence in the primal IT model presented here. This linkage implies that a vector of worst case scenario probabilities $\bar{\mathbf{p}}$ could be estimated relative to a reference distribution consistent with a historical or non-stressful period given an expected loss with the resulting estimate of the KL divergence providing a (now endogenous) measure of the scenario plausibility. This idea was originally suggested by B&C and is empirically explored below with reference to the BOG DFAST scenarios.

It is also the case that the optimal probabilities parameterized by $\theta = \bar{\theta}$ as in equation (4), when substituted into the primal Lagrangean equation (3) represent the unconstrained dual associated with the primal problem presented in (2). The dual is unconstrained because the partition function ensures the probabilities sum to one at $\theta = \bar{\theta}$ and therefore the probability summation equation is not needed. Making these substitutions, the Lagrangean is

$$\bar{\mathcal{L}} = \sum_{i=1}^n \bar{p}_i(\bar{\theta}) \ln \left(\frac{\bar{p}_i(\bar{\theta})}{p_i} \right) + \bar{\theta} \left(\mathbb{E}(l) - \sum_{i=1}^n \bar{p}_i(\bar{\theta}) l_i \right), \tag{7}$$

for the unconstrained dual. After substituting for the $\bar{p}_i(\bar{\theta})$ using (4) and simplifying, $\bar{\mathcal{L}} = \bar{\theta} \mathbb{E}(l) - \Lambda(\bar{\theta})$ results. Differentiating with respect to $\bar{\theta}$ yields the single FOC for an optimum of the dual problem, namely, $\mathbb{E}(l) - \Lambda'(\bar{\theta}) = 0$. Therefore, optimality implies that $\Lambda'(\bar{\theta})$ is the expected (maximum) loss as required by the MLT and shown in B&C.⁸

3 Empirical Examples

⁷ See equation (3) of Theorem 1 on page 1554 of Breuer and Csiszar (2013).

⁸ Maximum expected loss results because the dual optimization problem is a maximization problem. This is consistent with the primal optimization problem given in (2) as a minimization problem.

3.1 Example 1

Breuer and Csiszar's (2013) data⁹ are presented here as an example of the estimation of stressed default probabilities. The input data for their MLT method are given in the first two rows of Table 1 which show estimated percentage losses and historical transition probabilities over six possible credit ratings (i.e. $n = 6$). For comparison purposes, presented in the third row of Table 1 are the worst case scenario transition probabilities estimated by B&C (denoted \bar{p}_i (B&C)) while shown in the fourth and fifth rows of the table are the worst case scenario transition probabilities estimated using a numerical implementation of the MLT (fourth row) and the primal KL divergence IT model outlined above in (2) (fifth row). In the former case, $\bar{\theta}$ is estimated numerically given the data and the plausibility parameter $k = 2$ from which the \bar{p}_i are calculated as shown above in (4). In the latter case, the \bar{p}_i are estimated directly via the optimization problem in (2) above with the objective function value providing the estimate of k . As expected, the MLT and KL divergence IT models result in identical worst case scenario transition probabilities that are within rounding of the estimates reported by B&C.

Concentrating on the results associated with the MLT and KL divergence methods appearing in rows four and five in Table 1, the moment consistency equation implies the stressed expected loss, $\sum_{i=1}^n \bar{p}_i l_i = \mathbb{E}(l) = 18.74\%$ (compared to the historical or normal expected loss of $\sum_{i=1}^n p_i l_i = \mathbb{E}(l) = 0.36\%$) which is identical to the MLT estimate of the maximum loss given by $\Lambda'(\bar{\theta})$ when $\bar{\theta}=13.49$. As the parameter $\bar{\theta}$ is a multiplier for the moment consistency equation in the primal constrained optimization, the value shows the marginal impact on the objective function, in the IT case, KL divergence, from knowledge of the expected loss. With $\bar{\theta} > 0$, increasing $\mathbb{E}(l)$ increases KL divergence by inducing more stressed probabilities (i.e. more probability mass concentrated on the lower credit rating states). One additional set of worst case scenario probabilities is presented in the sixth row of Table 1 showing an expected loss $\mathbb{E}(l) = 32.42\%$. For this example, the estimated multiplier is $\bar{\theta} = 15.76$ while the objective function value (KL divergence) is 4.

As noted above, the MLT results are consistent with an exogenously specified $k=2$ whereas the primal IT model results in an estimate of KL divergence, \bar{D}^{KL} , equal to 2. The absolute worst case scenario for the data in this problem is one in which all the probability mass is concentrated on the state with the worst possible loss, namely the default state with an expected loss of 51.8%. This implies that the maximum value for k and hence the most stressful scenario

⁹ See Table 1 on p. 1556 of Breuer and Csiszar (2013).

for this specific problem and data has KL divergence equal to $\bar{D}^{KL} = \sum_i \bar{p}_i \ln\left(\frac{\bar{p}_i}{p_i}\right) = 1 \times \ln\left(\frac{1}{0.06\%}\right) = 7.4186$. Therefore, no feasible solutions to B&C's implementation of the MLT exist for scenarios defined by $k > 7.42$ because obligors default with certainty.

To summarize, the MLT requires an exogenous plausibility parameter, k , from which the multiplier $\bar{\theta}$ is estimated via the dual optimization problem. With the estimate of $\bar{\theta}$ in hand, stressed probabilities \bar{p}_i can be calculated directly as can the maximum expected loss $\mathbb{E}(l)$. The duality between the two entropic specifications implies that under the primal IT approach, it is $\mathbb{E}(l)$ that is exogenously specified with the stressed probabilities and multiplier $\bar{\theta}$ estimated directly by minimizing KL divergence. The estimate of KL divergence is the objective function value and precisely k , the plausibility parameter from the MLT.

One potential advantage of the dual approach is that portfolio managers can more easily articulate expected losses when conducting stress testing than they can scenario plausibility. In addition, there is a linkage between k and Value-at-Risk (VaR) α -significance according to the MLT. Namely, the maximum loss given by $\Lambda'(\bar{\theta})$ dominates Tail-VaR at the level $\exp(-k)$. This implies that, for example, 99 % VaR with $\alpha = 1\%$ implies $k = 4.61$ will create at least as stressful a scenario in terms of credit losses. While merely examples, these values provide much needed context for quantifying the extent of stress implicit in a choice of expected losses or the plausibility parameter. Further, they provide much needed context for assessing the plausibility of DFAST scenarios since each scenario has a time path of associated KL divergence that can be empirically measured.

3.2 Example 2

Having demonstrated the theoretical and empirical complementarity between the dual MLT and primal KL divergence methods, another example is presented here wherein estimated KL divergence is used to assess the extent to which two probability distributions differ. In a recent article by Varotto (2012), credit losses associated with historical stress scenarios are explored to determine whether regulatory capital and capital requirements under the so-called Basel 3 agreement suggest adequate protection. In Table 2 of Varotto (2012), Moody's credit migration matrices for corporate bonds and loans are presented under average (1921-2009), *Great Recession* (2008-09), *Great Depression* (1931-35), and worst case (1932) scenarios.

Mobility measures attributable to Jafry and Schuermann (2004) (JS) are also presented in Varotto (2012) and indicate that the increase in JS mobility is nearly (over) double for the *Great*

Recession (Great Depression) scenario relative to the average scenario. The worst case (i.e. 1932) scenario is suggestive of nearly a fourfold increase in JS mobility relative to the average scenario. Kullback-Leibler divergence can also be used to gauge the severity of a scenario since relative entropy by definition measures the extent of uncertainty or disorder in a distribution or system. More specifically, KL divergence is a measure of comparability between two probability distributions and is, therefore, a complementary measure to JS mobility.

Using the average migration matrix presented in Varotto (2012) as the reference distribution of transition probabilities, it follows that $D^{KL} = 0$ since there is no disorder in the average matrix relative to itself. Shown in Table 2 below are the transition probability and credit rating specific relative entropies for the three scenarios identified by Varotto (2012). Values in the table that are further from zero are indicative of more divergence between the two distributions and therefore, more stress relative to the average scenario. As shown in *Panel A*, the credit rating exhibiting the greatest disorder relative to the average for the *Great Recession* scenario (2008-09 average) is Aaa with an overall KL divergence of 0.1547. While the disorder associated with a reduction in the retention transition probability cannot be ignored, the main source of disorder stems from the transition probability associated with a downgrade from Aaa to Aa (0.2995). The remaining numbers can be interpreted similarly. Total KL divergence for the *Great Recession* scenario is also shown and suggests that $D^{KL} = 0.50$.

The preceding results are in contrast to the *Great Depression* scenario (1931-35 average) shown in *Panel B* of Table 2 wherein the most disorder appears to be related to the reduction in the retention probability, downgrade, and default of Ba, B, and Baa rated debt. Whereas most of the stress from the *Great Recession* appears to have been related to highly rated debt being downgraded, the *Great Depression* scenario was characterized more by the downgrade of less highly rated debt. Although not surprising, it is, however, also worth mentioning that the *Great Depression* scenario results in KL divergence equal to $D^{KL} = 0.7140 > 0.5053$ and obviously represents a more disordered or stressful scenario than the *Great Recession* scenario.

The *worst case* scenario (1932) shown in *Panel C* of Table 2 exhibits the greatest divergence of the three scenarios with an overall KL divergence equal to $D^{KL} = 3.3512$. The magnitude of this number alone is suggestive of how stressful the year 1932 was relative to the historical average. It should also be noted that approximately 40% of the total KL divergence in the *worst case* scenario stems from disorder associated with Baa rated debt downgrades and Ba rated debt downgrades and defaults. Even so, only about 10% of the total KL divergence for the

worst case scenario is attributable to Aaa and Caa-C rated debt implying that debt not rated high or low quality contributed significantly to the financial stress in 1932.

One caveat regarding the KL divergence estimates presented above for the *Great Recession* and *Great Depression* scenarios is that they are derived from probabilities that were averaged over the indicated number of years (2008-09 for the former and 1931-35 for the latter). This naturally has a smoothing effect that results in an understatement of the precise extent of the divergence. Presented in Table 3 are annual KL divergence estimates for Moody's and Fitch Global Corporate ratings for 2007 to 2013. For the Moody's ratings, average migration matrices from 1920-2013 and 1970-2013 are used as reference distributions while for the Fitch ratings, the period from 1990-2013 was used. In each case the KL divergence increases markedly in 2009 as global credit conditions deteriorated during the *Great Recession*.

Closer inspection of the estimated relative entropies of each rating class in Table 3 reveals that approximately 60% of the KL divergence in 2009 was due to Aaa to Aa (Moody's) and AAA to AA (Fitch) downgrades and transitions from Ca-C (Moody's) and CCC-C (Fitch) to the default state. Also shown in Table 3 is another indication of just how stressful the year 2009 was for credit markets. For the Moody's data, the maximum KL divergence for Ca to C rated debt is 1.23 (0.82) when using the 1920-2013 (1970-2013) average migration matrix as the reference distribution. As shown, calculated relative entropy for Ca to C rated debt is in excess of the maximum that would induce certain default. Overall, these estimates suggest that during normal times, $D^{KL} < 0.5$ on average and in the worst year of the *Great Recession* (i.e. 2009), $D^{KL} \geq 1$ suggesting divergence spiked to levels around one (Fitch) or higher (Moody's). By contrast, the worst year of the *Great Depression* (i.e. 1932), $D^{KL} > 3$ using Varotto's (2013) data. These values provide some context for the analysis and results presented below. As an aside, the handpicked scenario reported by Miu and Ozdemir (2009) and described above results in $D^{KL} = 0.92$ which is of a magnitude that is reasonably consistent with the *Great Recession* scenario.

4 Severity of DFAST Scenarios

The preceding examples demonstrate how KL divergence can be empirically estimated and used as a measure of the disorder or the extent of divergence between two empirical probability distributions. The relative entropy approach applied to measure the extent of stress implied by DFAST then requires an estimate of a joint distribution of macroeconomic factors using, for

example, historical data from which the KL divergence can be estimated under each DFAST scenario using the IT approach discussed previously. The most recent DFAST scenarios were released by the Federal Reserve in October 2014 for a total of 16 domestic macroeconomic variables and 12 international variables. Shown in Table 4 is a list of the domestic macroeconomic variables along with short descriptions of the variables and data sources. These data consist of six measures of economic activity and prices, four aggregate measures of asset prices or financial conditions, and six measures of interest rates.

Shown in Figures 1 and 2 are phase diagrams depicting historical and scenario driven paths for several of the domestic DFAST macroeconomic variables. In most cases, it appears that the base and adverse scenarios are more or less what one would expect given their descriptions. For example, all four panels show base scenarios that are well within the confines of the historical movement of each of the variables. Similarly, the adverse scenarios shown in each of the panels depart significantly from history when compared to the base scenarios, but in general appear to be visually stressful while not implausible.

The severely adverse scenario, however, appears to be quite stressful in that it suggests departures from historical levels that, at least visually, appear to be fairly significant. Perhaps more importantly, as shown, the departures are for extensive periods of time. For example, in Panel A of Figure 1, significant negative nominal GDP growth is shown for the severely adverse scenario in conjunction with nominal 10-year treasury yields that are also quite low. Highlighted in Panel A of Figure 1 are Q4: 2008 and Q1: 2009 for reference showing lower levels of nominal GDP growth at considerably higher levels of nominal 10-year Treasury yields. Similarly, nominal 10-year treasury yields are shown in Panel B of Figure 1 relative to the commercial real estate index. Again, the severely adverse scenario appears to depart significantly from the historical data but also does so for an extended period of time. Perhaps the most striking depiction is shown in Panel A of Figure 2 where the VIX index is plotted against nominal year-over-year growth in the Dow Jones index. As shown, the severely adverse scenario is fully outside the bounds of the historical data going back to 1990, the first year for the VIX.

Using data for a slightly longer time period, unemployment and year-over-year growth in nominal GDP are shown in Panel B of Figure 2. In this case the severely adverse scenario mimics the phase path of late 2008 into early 2009 albeit at a significantly higher level of unemployment (8-10% rather than 6-8%). The recovery from this scenario appears to split the difference between the paths associated with GDP growth and unemployment in 2009 (below the severely adverse

scenario path) and the phase path associated with the late 1982 to early 1983 recovery period (above the severely adverse scenario path).

While there is no finite set of macroeconomic variables that can provide a perfect characterization of the economy, the variables listed in Table 4 can likely provide an adequate characterization for the purposes of determining the inherent level of stress implied by DFAST scenarios. As a practical matter, the estimation of a joint density necessitates careful consideration of only a few variables given the numerical intensity of the process. Therefore, a subset of the macroeconomic variables in Table 4 consisting of the real rate of growth in GDP, the unemployment rate, real 10-year Treasury yields, and the real rate of growth in the Dow Jones index were used to estimate the joint distribution.

To arrive at this subset of variables, the international variables were explicitly ignored and real values were deemed preferable to nominal values thereby eliminating the nominal GDP and disposable income growth variables. The six interest rates are all highly correlated so the 10-year Treasury yield was chosen as representative due also to its importance for residential and commercial real estate lending. The effects of the equity market are accounted for by the selection of the Dow Jones index which was subsequently converted to a rate of growth. The volatility index was eliminated from consideration due to its low rate of use in stress testing according to Fender *et al.* (2001).¹⁰ Treasury yields and the rate of growth in the Dow were converted to real rates using the DFAST Consumer Price Index macroeconomic variable.

Shown in Figure 3 are the (recent) historical and scenario paths for the real rate of growth in GDP, unemployment rate, the real yield on 10-year Treasuries, and the real rate of growth in the Dow Jones industrial average.¹¹ The three scenarios: baseline, adverse, and severely adverse are also shown for the last quarter of 2014 and the two subsequent years and represent the BOG's quarterly value for this macroeconomic variable under each DFAST scenario. Again, it appears that the baseline scenario is a fairly benign scenario while the adverse scenario injects what appears to be a plausible amount of stress. The severely adverse scenario however, appears to be characterized by a considerable amount of stress for a relatively long period of time. Whether these scenarios and their duration are plausible is the topic of this section.

¹⁰ It is likely that a model that includes the VIX increases KL divergence considerably given the phase paths shown in Panel A of Figure 2.

¹¹ Recall, the 10-year Treasury yield was converted to a real rate and the Dow Jones Stock Market Index was converted to a real rate of growth. Subsequently, the base, adverse, and severely adverse values for both variables had to be converted as well using the BOG's DFAST CPI value under each scenario.

4.1 Joint Density Estimation

The pure inverse IT optimization problem with zero moments shown above in (2) can be used to estimate the KL divergence of a given DFAST scenario by estimating the probabilities according to the general IT econometric problem

$$\begin{aligned}
 \mathbf{p}^* &= \operatorname{argmin}\{D^{KL}(\mathbf{p} \parallel \mathbf{q}^*)\} \\
 \text{s.t.} \\
 f_m(\mathbf{y}, \mathbf{x}, \mathbf{p}) &= [\mathbf{0}], m = 1, 2, \dots, M \\
 \mathbf{p}'\mathbf{1} &= 1 \\
 \mathbf{p} &\geq \mathbf{0}.
 \end{aligned} \tag{8}$$

Here, the elements of \mathbf{p} make up the discrete joint density and are chosen relative to the discrete joint (reference) density defined by \mathbf{q}^* subject to M moment consistency equations, adding up, and non-negativity constraints. Notice that there is one moment consistency equation for each DFAST macroeconomic factor for each of the three BOG scenarios. With four macroeconomic factors, the estimation of the discrete probabilities, p_{ijkl} , in (8) is conducted a total of 39 times; once for each of the 13 quarters making up each of the three BOG scenarios.

However, before estimating (8), the joint reference density, \mathbf{q}^* , must be estimated. Empirical (marginal) distributions for each of the four macroeconomic factors discussed above were initially analyzed by fitting a histogram to each variable using historical data. The estimated histograms are presented in Figure 4 with the summary statistics presented in Table 5. The bin size and hence the bin width for each histogram was determined by optimizing the L^2 risk function as in Shimazaki and Shinomoto (2007). In each case, the data shown on the x -axis for each histogram are the midpoints of the bins and also serve as the parameter supports for the estimation of the joint reference density, \mathbf{q}^* , as well as the joint density, \mathbf{p} , in (8).

As shown in the bottom of Table 5, the macroeconomic variables are not independent and the estimation of \mathbf{q}^* should accommodate this feature of the data. One way of capturing the (linear) correlation structure is to specify second (central or non-central) moment equations in addition to the moment consistency equations typical of IT estimation. The resulting model is likely a stochastic IT optimization since the inclusion of higher moments make it increasingly difficult to match all the moments without error with a given set of data. The following generalized IT model is used to estimate the reference joint density, \mathbf{q}^* , by assuming first, second, and cross moment consistency

$$\begin{aligned}
\max D(\mathbf{q}, \mathbf{u}, \mathbf{w}) &= -\mathbf{q}' \ln \mathbf{q} - \mathbf{u}' \ln \mathbf{u} - \mathbf{w}' \ln \mathbf{w} \\
\text{s.t.} & \\
&\mathbf{q}' \mathbf{x} + \mathbf{u}' \mathbf{v} = \hat{\boldsymbol{\mu}} \\
&\mathbf{q}' \mathbf{x}^2 + \mathbf{w}' \mathbf{z} = \hat{\boldsymbol{\Sigma}} \\
&\mathbf{q}' \mathbf{1} = 1, \mathbf{u}' \mathbf{1} = 1, \mathbf{w}' \mathbf{1} = 1 \\
&\mathbf{u}' \mathbf{v} = 0, \mathbf{w}' \mathbf{z} = 0 \\
&\mathbf{q} \geq 0, \mathbf{u} \geq 0, \mathbf{w} \geq 0.
\end{aligned} \tag{9}$$

Here, total entropy is measured over the distribution of \mathbf{q} as well as the vector of probabilities \mathbf{u} and matrix \mathbf{w} appearing in the various moment equations. There are a total of four moment consistency equations made up of a vector of parameter supports, \mathbf{x} , a matrix of error probabilities, \mathbf{u} , an error support vector, \mathbf{v} , and a vector of (exogenous) empirical means, $\hat{\boldsymbol{\mu}}$. As noted above, the vector of parameter supports are shown along the x -axis in each histogram in Figure 5 while the vector of empirical means is shown in Table 5. The error support vector consists of positive and negative elements such that the sum-product of the error supports and estimated error probabilities yields a vector of errors that ensure a feasible solution can be found. Additionally, the errors constructed by $\mathbf{u}' \mathbf{v}$ are centered on zero (i.e. mean zero) as indicated by the constraints.

The second and cross moments for each variable are matched with the empirical matrix of second and cross moments, $\hat{\boldsymbol{\Sigma}}$, (shown in Table 5) by optimally choosing the \mathbf{q} and the matrix of (error) probabilities \mathbf{w} given an error support vector, \mathbf{z} . As above, the error support vector \mathbf{z} has both positive and negative elements that ensure a feasible solution can be found while the errors constructed by $\mathbf{w}' \mathbf{z}$ are mean zero. The remaining equations simply ensure that all the probabilities are proper (i.e. non-negative and sum up to unity). While the estimation of the reference distribution as in (9) is a critical input to the estimation of the KL divergence, $D^{KL}(\mathbf{p} \parallel \mathbf{q})$, appearing in (8), the results of the estimation of \mathbf{q} are not presented here.¹² More details on the density estimation in (9) appear in Appendix 1 and the specific 4-factor version of the IT estimation (8) in Appendix 2.

4.2 DFAST Scenario Severity

¹² The dimensions of the parameter support space as shown in the histograms in Figure 4 suggests that the optimal \mathbf{q}^* has 76,032 probabilities not including the probabilities associated with the error terms appearing in the moment equations in (10).

As noted above, the DFAST scenarios are not meant to be taken as BOG forecasts, but rather plausible scenarios consistent with a baseline and two increasingly stressful alternatives. According to the BOG, the supervisory baseline scenario resembles the average predictions from surveyed forecasters and shows a moderate expansion in economic activity, with modest real GDP growth, modestly increasing equity, residential, and commercial real estate prices, decreasing unemployment, a gradual normalization of treasury yields, and low market volatility. The supervisory adverse scenario is characterized by a global weakening in economic activity resulting in a mild recession, falling equity, residential, and commercial real estate prices, increased inflation, and a rapid increase in treasury yields. The primary difference between the 2015 adverse scenario and the 2014 adverse scenario is the latter's suggestion of a steepening of the yield curve as opposed to an overall lifting of the curve. Finally, the supervisory severely adverse scenario contemplates a deep and prolonged U.S. recession, with high unemployment and real GDP declining substantially. Treasury rates remain low, while equity, residential and commercial real estate prices fall dramatically and exhibit substantial volatility.

Shown in Table 6 are the time paths for estimated KL divergence for each quarter and scenario found by estimating the probabilities as described above using the IT estimation (8). The estimated $D^{KL}(\mathbf{p}^* \parallel \mathbf{q}^*) = D^{KL*}$ are plotted in the first three panels of Figure 5 along with the estimated D^{KL*} from assuming that the joint distribution of macroeconomic variables is independent.¹³ As shown, the base scenario is quantified as more or less how the BOG describes the scenario, namely a benign scenario with low KL divergence. Recall, KL divergence near zero is indicative of a distribution of stressed probabilities that differ only mildly from the reference distribution. As shown in Figure 5, the estimated KL divergence for each scenario is higher when the correlation between the macroeconomic variables is taken into account. Also, the base scenario has KL divergence that generally decreases over the relevant quarters regardless of the correlation between the macroeconomic variables.

Given the magnitude of the estimated D^{KL*} the adverse scenario appears to offer a plausible level of stress while the severely adverse scenario is consistent with a considerably higher level of stress that may not even be plausible. As shown in Panel B of Figure 5, the mild recession that characterizes the adverse scenario results in KL divergence that peaks around 1.0 (correlated) and 1.4 (independent) and steadily falls over the remaining quarters making up the scenario.

¹³ If the macroeconomic factors are independent, the joint probabilities are simply the product of the marginal probabilities. As shown in Schönbucher (2003), this is also analogous to the independence copula.

For comparison, recall that the *Great Recession* scenario as presented above suggests that $D^{KL*} \geq 1$ as credit conditions worsened.¹⁴ By contrast, recall that the worst year of the *Great Depression* scenario resulted in an estimate of $D^{KL*} = 3.35$. As shown, the severely adverse scenario has KL divergence in excess of 3.35 until Q4 2015. Even so, the severely adverse scenario has an extreme amount of stress over the first year that eventually only settles to around $D^{KL*} \approx 2$. As an additional point of reference, using B&C's model and data, it was noted above that a total portfolio loss (i.e. all probability mass centered on the default state) would result in KL divergence of 7.42. The BOG's severely adverse scenario has the first three quarters around this level with the first quarter of 2015 well in excess implying default with certainty.

To further add some context to the estimated KL relative entropies, shown in Panel D of Figure 5 are the expected (maximum) loss curves found by applying the MLT of B&C using the estimated KL relative entropies shown in Table 6. As shown, an application of the base and adverse scenarios would result in credit losses of less than 5% (base) and 12% (adverse) that generally decrease over time to less than 10% for both scenarios. By contrast, the severely adverse scenario implies much higher credit losses. The severely adverse scenario has an infeasible level of expected credit losses given the KL divergence for the first quarter of 2015 ($D^{KL*} = 8.36 > 7.42$). Nonetheless, the expected credit losses are about 50% until Q4 2015 when they drop to and stabilize around 25% before subsequently dropping to around 15% by the end of 2017.

Shown in Table 7 are the shadow prices for each of the moment consistency equations in each quarter under each scenario. The reported values are relative entropies, that is, the relative contribution of each data point-constraint to the optimal objective function value. Consequently, the multipliers reflect the information content of each constraint. Since the constraints of the model represent the expected value of each of the macroeconomic variables, the multipliers give an indication of the impact on KL divergence from a marginal change in each expectation. For example, the unemployment rate has negative (positive) multipliers for every quarter under the adverse and severely adverse (base) scenarios. Since the model is oriented toward minimization, these estimates suggest that marginal increases in the BOG's projection of the expected unemployment rate will lead to higher (lower) KL divergence or more simply, more (less) stress under the adverse and severely adverse (base) scenarios. Of particular note is the magnitude of multipliers under the severely adverse scenario during the latter half of 2015 through much of

¹⁴ Recall also that the example handpicked stress scenario presented in Miu and Ozdemir (2009) had $D^{KL*} = 0.92$

2016. From Panel B of Figure 3 it can be seen that unemployment peaks around this time and remains at this exceptionally high level for much of the duration of the scenario.

From these results it is clear that the baseline scenario is not at all stressful and is more or less consistent with the BOG's description as a scenario characterized by historical levels for the macroeconomic variables modeled. By contrast the adverse scenario induces an elevated level of stress whereby expected losses are likely to ramp up considerably but not necessarily to unrealistic or implausible levels. In fact, the adverse scenario may not induce quite the level of stress that was experienced during the *Great Recession*. However, the severely adverse scenario, mostly by virtue of the fact that the stress is so pervasive and unrelenting, may be too stressful for practical use. It is possible that the level and perhaps more importantly the duration of stress implied by the severely adverse scenario causes substantive structural changes in the underlying economy that are not likely to be accounted for in any stress testing model developed by an institution and conditioned on historical data. For example, Q1 2015 may be suggestive of a level of stress that induces certain default. What happens after a significant number of institutions all experience certain default by obligors making up their portfolios is not altogether clear.

4.3 *Non-BOG Macroeconomic Variables*

Another use of the KL divergence approach outlined above is to use a variant of the IT estimator in (10) to generate data for use in stress testing models that is consistent with the level of stress implied by the BOG scenarios. For some financial institutions the linkage between the specific macroeconomic factors prescribed by the BOG and the institution's portfolio may be tenuous at best. For example, a Midwestern commercial bank or perhaps a Farm Credit System bank with significant farm real estate exposure would have somewhat limited prospects for tying loan balances, losses, or credit rating migrations to any of the macroeconomic variables other than perhaps the 10-year Treasury yield.¹⁵ While the 10-year Treasury yield is known to correlate positively with commercial and agricultural mortgage rates as well as negatively with farm real estate values, it is farm real estate values that would be of most interest for a bank with farm real estate exposure. While such institutions have the flexibility and authorization to choose farm real estate values as an appropriate macroeconomic factor, there are no scenario values put forth by the BOG for such a variable.

¹⁵ The Farm Credit System is comprised of a network of cooperative lenders that have the largest share of loans collateralized by farm real estate in the U.S.

Left with this, historical and/or handpicked scenarios would likely be used. A relatively simple extension of the methods presented previously is developed here to demonstrate how KL divergence can be used to identify stress levels consistent with the BOG scenarios or at least help calibrate handpicked scenarios. First, the joint distribution of quarterly cash corn prices in Iowa and farm real estate growth rates are estimated using the IT estimator presented in (10). Since most farm real estate in Iowa is consistent with high quality land, cash rents and hence growth rates in value are positively related to the price of corn, an easily observed economic variable. The farm real estate growth rates used in this exercise are the District 7 growth rates reported quarterly by the Chicago Federal Reserve. Shown in Figures 6 and 7 for comparison purposes are joint densities assuming independence (Figure 6) and positive correlation (Figure 7) between the two variables. In the latter case, the empirical second and cross moments were matched as a part of the estimation to accommodate the historical positive correlation of 0.18 between the two variables.

Using the joint density in Figure 8 as the reference distribution (ω) and varying the levels of the two variables over their empirical ranges results in the KL divergence surface presented in Figure 9. Using data going back to 1965, the empirical mean District 7 growth rate (Iowa cash corn price) is 1.94% (\$2.50/bu). As shown in Figure 8, the KL divergence is minimized around these mean values with more extreme values giving rise to higher levels of KL divergence. Sampling growth rates and corn prices from areas on the KL divergence surface that matches the BOGs scenario KL divergence would allow a bank to use levels for these variables that are consistent with the BOGs scenarios.

As an example, an adverse scenario with $D^{KL}(\mathbf{p}^* \parallel \mathbf{q}^*) \approx 1$ suggests that appropriate variable values could come from a variety of areas along the surface in Figure 8. Notice that the type of lending will determine whether a given scenario will consist of high or low corn prices. For example, a stress scenario defined by a decline in land values for a crop producer would suggest low land value growth rates values and low corn prices while stress for an integrated swine producer might consist of low land growth rates and high corn prices. The approach is flexible enough to handle either case.

5 Conclusions

Since the passage of the Dodd Frank Wall Street Reform and Consumer Protection Act, many financial institutions have been developing and validating stress testing models and methodologies in preparation for annual and semi-annual stress testing. However, to date little is known about the extent of the stress implied by the scenarios prescribed by regulators. In this paper, Kullback-Leibler divergence is suggested as a mechanism to assess how much stress is implied by each scenario by measuring the extent that regulators' scenarios differ from historical standards.

The results of the analysis presented here show that the regulator's baseline scenario is more or less as advertised. That is, a rather benign scenario that induces very little stress compared to historical standards. The other two scenarios induce more stress with the severely adverse scenario consistent with considerable stress. By way of historical comparison, the adverse scenario appears to be somewhat comparable to levels of stress consistent with at least the recent recession. By contrast, the severely adverse scenario likely induces a level of stress that may be considerably worse than the worst year of the *Great Depression*. The severely adverse scenario may actually be consistent with such an unprecedented level of stress that it may actually undermine its usefulness as a plausible scenario for use in stress testing.

For financial institutions with exposure to industries or sectors of the economy that cannot be readily linked back to the DFAST macroeconomic variables, KL relative entropy may be especially useful. For a set of macroeconomic variables that make more sense for these types of institutions than the DFAST macroeconomic variables, projecting quarterly values with relative entropy consistent with the DFAST scenarios is relatively straightforward.

Additional research should be directed along at least two dimensions. First, other (perhaps larger) subsets of macroeconomic variables could be explored to see whether better characterizations of the joint density are possible. For example, a large bank with an international footprint would need to see a characterization of the macro-economy that includes some of the international economic variables that are a part of the regulator's scenario projections. In addition, alternative characterizations of the correlation structure in the estimation of the joint density may offer improvement the methods presented here. The severely adverse scenario is an extremely stressful scenario and it may be the case that under such levels of stress, the correlation between the macroeconomic variables is strengthened as a result. The impact of such nonlinear correlation could be captured by measuring the extent of KL divergence from a copula estimated joint density.

References

- Abdymomunov, A., and Gerlach, J., 2014. Stress testing interest rate risk exposure. *Journal of Banking and Finance* 49, 287-301.
- Agmon, N., Alhassid, Y., and Levine, R., 1979. An algorithm for finding the distribution of maximal entropy. *Journal of Computational Physics* 30, 250-59.
- Alexander, C., and Sheedy, E., 2008. Developing a stress testing framework based on market risk models, *Journal of Banking and Finance* 32, 2220-2236.
- Balasubramnian, B., and Cyree, K., 2014. Has market discipline on banks improved after the Dodd-Frank act? *Journal of Banking and Finance* 41, 155-166.
- Bangia, A., Diebold, F., Kronimus, A., and Schagen C., 2002. Ratings migration and the business cycle, with application to credit portfolio stress testing, *Journal of Banking and Finance* 26, 445-474.
- Berger, A., and Bouwman, C., 2013. How does capital affect bank performance during financial crises? *Journal of Financial Economics* 109, 146-176.
- Board of Governors of the Federal Reserve System, 2014 Supervisory scenarios for annual stress tests required under the Dodd-Frank act stress testing rules and the capital plan rule, November 1, 2013.
- Breuer, T., 2008. Overcoming dimensional dependence of worst case scenarios and maximum loss, *Journal of Risk* 2, 115-136.
- Breuer, T., and Csiszar, I., 2010. If worse comes to worst: systematic stress testing in general risk models. eLibrary 1328022, SSRN <[hyyp://ssrn.com/paper=13328022](http://ssrn.com/paper=13328022)>.
- Breuer, T., and Csiszar, I., 2013. Systematic stress tests with entropic plausibility constraints. *Journal of Banking and Finance* 37, 1552-1559.
- Breuer, T., Jandacka, M., Rheinberger, K., and Summer, M., 2009. How to find plausible severe and useful stress scenarios. *International Journal of Central Banking* 3, 205-224.
- Breuer, T., Jandacka, M., Mencia, J., and Summer, M., 2012. A systematic approach to multi-period stress testing of portfolio credit risk, *Journal of Banking and Finance* 36, 332-340.
- Cressie, N., and Read, T., 1984. Multinomial goodness-of-fit tests. *Journal of the Royal Statistical Society B* 46, 440-464.
- Committee on the Global Financial System. 2005. Stress testing at major financial institutions: survey results and practice. Bank for International Settlements.

- Dodd, C., and Frank, B., 2010. Dodd–Frank wall street reform and consumer protection act, Pub.L. 111–203, H.R. 4173.
- Fender, I., Gibson, M., and Mosser, P., 2001. An International Survey of Stress Tests. *Current Issues in Economics and Finance* 7(10), Federal Reserve Bank of New York.
- Golan, A., 2002. Information and entropy econometrics – editor’s view. *Journal of Econometrics* 107, 1-15.
- Golan, A., 2006. Information and entropy econometrics – a review and synthesis. *Foundation and Trends in Econometrics* 2, 1-145.
- Huang, X., Zhou, H., and Zhu, H., 2009. A framework for assessing the systematic risk of major financial institutions, *Journal of Banking and Finance* 33, 2036-2049.
- Imbens, G., Spady, R., and Johnson, P., 1998. Information theoretic approaches to inference in moment condition models, *Econometrica* 66, 333-357.
- Jafry, Y., and Schuermann, T., 2004. Measurement, estimation and comparison of credit migration matrices. *Journal of Banking and Finance* 28, 2603-2639.
- Kitamura, Y., and Stutzer, M., 1997. An Information-theoretic alternative to generalized method of moments estimation, *Econometrica* 65, 861-874.
- Kullback, S., and Leibler, R., 1951. On information and sufficiency. *Annals of Mathematical Statistics* 22, 79–86.
- Miu, P., and Ozdemir, B., 2009. Stress-testing probability of default and migration rate with respect to Basel II requirements, *Journal of Risk Model Validation* 3, 3-38.
- Rényi, A., 1961. On measures of entropy and information. In *Proceedings of the 4th Berkeley Symposium on Mathematical Statistics and Probability, Volume I*, Berkeley: University of California Press, 547-561.
- Schönbucher, P., 2003. *Credit derivatives pricing models*. John Wiley and Sons Ltd., West Sussex, England.
- Shannon, C., 1948. A mathematical theory of communication. *Bell System Technical Journal* 27, 379-423; 623-565.
- Shimazaki, H., and Shinomoto, S., 2007. A method for selecting the bin size of a time histogram. *Neural Computation* 19, 1503–1527.
- Varotto, S., 2012. Stress testing credit risk: the great depression scenario. *Journal of Banking and Finance* 36, 3133-3149.

Wu, X., 2003. Calculation of maximum entropy densities with application to income distribution, *Journal of Econometrics* 115, 347-354.

Zellner, A., and Highfield, R., 1988. Calculation of maximum entropy distributions and approximation of marginal posterior distributions. *Journal of Econometrics* 37, 195-209.

Appendix 1

Univariate and Multivariate Density Estimation

Let $\mathbf{x} = [x_1, x_2, \dots, x_n]$ be a parameter support vector for a single macroeconomic variable and $\mathbf{q} = [q_1, q_2, \dots, q_n]$ be a discrete distribution of probabilities to be estimated. The univariate probability density function estimation cast as a primal constrained optimization IT with non-central moments is

$$\begin{aligned} \max D(\mathbf{q}) &= - \sum_i q_i \ln q_i \\ \text{s.t.} \\ \sum_{i=1}^n q_i x_i^k &= \mu_k, \quad \forall k = 0, 1, \dots, m \\ q_i &\geq 0, \quad \forall i \end{aligned} \tag{A.1}$$

where $\mu_0 = 1$. Zellner and Highfield (1988) discuss such an approach and conduct estimation with $m = 4$. Wu (2003) reports on the efficiency of a model similar to that presented in (A.1) for the estimation of the distribution of U.S. income where the moments are updated sequentially rather than simultaneously.

Extending the model presented above to the simplest possible multivariate case (i.e. two variables) yields

$$\begin{aligned} \max D(\mathbf{q}) &= - \sum_i \sum_j q_{ij} \ln q_{ij} \\ \text{s.t.} \\ \sum_i \sum_j x_i^k y_j^h &= \mu_{kh}, \quad \forall k = 0, 1, \dots, K, h = 0, 1, \dots, H \\ q_{ij} &\geq 0, \quad \forall i, j \end{aligned} \tag{A.2}$$

where $\mu_{00} = 1$.¹⁶

¹⁶ It is not likely that all the moment conditions can be met with strict equality with empirical data. In such cases, error terms can be added to the moment equations such as $\varepsilon = \mathbf{u}\mathbf{v}'$ where $\mathbf{v}' = [v_1, v_2, \dots, v_n]$ is an error support vector and $\mathbf{u} = [u_1, u_2, \dots, u_n]$ is a probability distribution with $\sum_n u_n = 1$ added as a constraint. The estimation then involves finding the vector \mathbf{u} as well as the vector \mathbf{q} after adding $-\sum_j u_j \ln u_j$ to the objective function. To ease the notion associated with the current model, these features are left out of the model exposition.

Let θ_{kh} denote the k th- h th multiplier and assuming $K = H = 2$ (i.e. first and second moments and cross moments), the Langrangian for the system (A.2) is

$$\mathcal{L} = -\sum_i \sum_j q_{ij} \ln q_{ij} + \sum_k \sum_h \theta_{kh} \left(\sum_i \sum_j q_{ij} x_i^k y_j^h - \mu_{kh} \right) \quad (\text{A.3})$$

The necessary conditions for an optimum consist of the nine constraints in (A.2) (since there are two variables and moments and cross moments up to second order) plus the following n^2 equations

$$-1 - \ln q_{ij} + \sum_k \sum_h \theta_{kh} \left(\sum_i \sum_j x_i^k y_j^h - \mu_{kh} \right) = 0 \quad \forall i, j = 1, \dots, n. \quad (\text{A.4})$$

Here, it is assumed there are n data points for each of the two variables and therefore n^2 probabilities, q_{ij} to be estimated. From (A.4), the optimal probabilities, q_{ij}^* , can be analytically expressed as a nonlinear function of the optimized Lagrange multipliers, θ_{kh}^* , namely

$$q_{ij}^* = \exp \left[\sum_k \sum_h \theta_{kh}^* \left(\sum_i \sum_j x_i^k y_j^h - \mu_{kh} \right) - 1 \right]. \quad (\text{A.4})$$

Given the nonlinearity inherent in (A.4), numerical procedures must be used to estimate the set of probabilities that simultaneously solve the $n^2 + 9$ first-order conditions.

Appendix 2

4-factor DFAST KL Divergence IT Estimation

The 4-factor stressed joint density estimation cast as a discrete primal constrained optimization IT problem with KL divergence is

$$\begin{aligned}
 \min \mathbf{D}^{KL}(\mathbf{p} \parallel \mathbf{q}^*) &= \sum_{i \in I} \sum_{j \in J} \sum_{k \in K} \sum_{l \in L} p_{ijkl} \ln \left(\frac{p_{ijkl}}{q_{ijkl}^*} \right) \\
 \text{s.t.} & \\
 \sum_{i \in I} g_i \left(\sum_{j \in J} \sum_{k \in K} \sum_{l \in L} p_{ijkl} \right) &= \hat{g} \\
 \sum_{j \in J} u_j \left(\sum_{i \in I} \sum_{k \in K} \sum_{l \in L} p_{ijkl} \right) &= \hat{u} \\
 \sum_{k \in K} y_k \left(\sum_{i \in I} \sum_{j \in J} \sum_{l \in L} p_{ijkl} \right) &= \hat{y} \\
 \sum_{l \in L} d_l \left(\sum_{i \in I} \sum_{j \in J} \sum_{k \in K} p_{ijkl} \right) &= \hat{d} \\
 \sum_{i \in I} \sum_{j \in J} \sum_{k \in K} \sum_{l \in L} p_{ijkl} &= 1 \\
 p_{ijkl} &\geq 0, \forall i, j, k, l
 \end{aligned} \tag{B.1}$$

Here, we seek a vector of discrete probabilities p_{ijkl} relative to the reference distribution of probabilities q_{ijkl}^* that minimize the KL divergence subject to four moment consistency equations, an adding up equation that ensures the total density sums to one, and non-negativity constraints for the probabilities. The q_{ijkl}^* are found in a first stage estimation of the model in Appendix 1. For the moment consistency equations, g_i represents the i th value of a parameter support vector for the real rate of growth in GDP such as $\mathbf{g} = [g_1, g_2, \dots, g_I]'$ so that the expected value, $\mathbf{g}'\mathbf{p}$, equals the (exogenous) GDP growth suggested by the Fed under a given scenario and denoted above as \hat{g} . The parameter support vectors for the unemployment rate, \mathbf{u} , real 10-year Treasury yield, \mathbf{y} , and real rate of growth in the Dow Jones industrial average, \mathbf{d} , are defined analogously.

The Langrangian for this pure inverse problem is

$$\begin{aligned}
\mathcal{L} = & \sum_i \sum_j \sum_k \sum_l p_{ijkl} \ln \left(\frac{p_{ijkl}}{q_{ijkl}^*} \right) + \theta_g \left[\hat{g} - \sum_i g_i \left(\sum_j \sum_k \sum_l p_{ijkl} \right) \right] \\
& + \theta_u \left[\hat{u} - \sum_j u_j \left(\sum_i \sum_k \sum_l p_{ijkl} \right) \right] \\
& + \theta_y \left[\hat{y} - \sum_k y_k \left(\sum_i \sum_j \sum_l p_{ijkl} \right) \right] \\
& + \theta_d \left[\hat{d} - \sum_l d_l \left(\sum_i \sum_j \sum_k p_{ijkl} \right) \right] + \gamma \left(1 - \sum_i \sum_j \sum_k \sum_l p_{ijkl} \right),
\end{aligned} \tag{B.2}$$

from which there are $I \times J \times K \times L + 5$ first-order conditions (FOCs), namely,

$$\begin{aligned}
\frac{\partial \mathcal{L}}{\partial p_{ijkl}} &= 1 + \ln \left(\frac{p_{ijk}}{q_{ijkl}^*} \right) - \theta_g g_i - \theta_u u_j - \theta_y y_k - \theta_d d_l - \gamma, \quad \forall i, j, k, l \\
\frac{\partial \mathcal{L}}{\partial \theta_g} &= \hat{g} - \sum_i g_i \left(\sum_j \sum_k \sum_l p_{ijkl} \right) \\
\frac{\partial \mathcal{L}}{\partial \theta_u} &= \hat{u} - \sum_j u_j \left(\sum_i \sum_k \sum_l p_{ijkl} \right) \\
\frac{\partial \mathcal{L}}{\partial \theta_y} &= \hat{y} - \sum_k y_k \left(\sum_i \sum_j \sum_l p_{ijkl} \right) \\
\frac{\partial \mathcal{L}}{\partial \theta_d} &= \hat{d} - \sum_l d_l \left(\sum_i \sum_j \sum_k p_{ijkl} \right) \\
\frac{\partial \mathcal{L}}{\partial \gamma} &= 1 - \sum_i \sum_j \sum_k \sum_l p_{ijkl}.
\end{aligned} \tag{B.3}$$

The simultaneous solution to the first $I \times J \times K \times L$ FOCs are required to minimize KL divergence implying that

$$p_{ijkl}^* = q_{ijkl}^* \exp(\theta_g^* g_i + \theta_u^* u_j + \theta_y^* y_k + \theta_d^* d_l + \gamma^* - 1), \quad \forall i, j, k. \tag{B.4}$$

where the stars denote optimized values of the Lagrange multipliers. The solutions to these FOCs may be written as

$$p_{ijkl}^* = \frac{q_{ijkl}^* \exp(\theta_g^* g_i + \theta_u^* u_j + \theta_y^* y_k + \theta_d^* d_l)}{\Omega(\boldsymbol{\theta}^*; \mathbf{p}^*)}, \quad \forall i, j, k. \tag{B.5}$$

where

$$\Omega(\boldsymbol{\theta}^*; \mathbf{p}^*) = \sum_i \sum_j \sum_k \sum_l p_{ijkl}^* \exp(\theta_g^* g_i + \theta_u^* u_j + \theta_y^* y_k + \theta_d^* d_l) \quad (\text{B.6})$$

is a partition function that converts the relative probabilities to absolute probabilities. The Lagrange multipliers on the moment consistency constraints are determined by the solution to the four simultaneous equations

$$\hat{g} = \frac{\partial \ln \Omega(\boldsymbol{\theta}; \mathbf{p})}{\partial \theta_g}, \hat{u} = \frac{\partial \ln \Omega(\boldsymbol{\theta}; \mathbf{p})}{\partial \theta_u}, \hat{y} = \frac{\partial \ln \Omega(\boldsymbol{\theta}; \mathbf{p})}{\partial \theta_y}, \hat{d} = \frac{\partial \ln \Omega(\boldsymbol{\theta}; \mathbf{p})}{\partial \theta_d}. \quad (\text{B.7})$$

Given the Lagrangean and the FOCs above, it follows that

$$\frac{\partial^2 \mathcal{L}}{(\partial p_{ijkl}^*)^2} = (p_{ijkl}^*)^{-1}, \quad (\text{B.8})$$

along the diagonal and zero otherwise. Therefore, the Hessian matrix for \mathcal{L} is given by

$$\mathbf{H}_{\mathcal{L}} = \begin{bmatrix} 1/p_{1111}^* & \cdots & 0 \\ \vdots & \ddots & \vdots \\ 0 & \cdots & 1/p_{IJKL}^* \end{bmatrix}, \quad (\text{B.9})$$

and is positive definite for $p_{ijkl}^* > 0$ ensuring a unique global minimum.

Table 1. Breuer and Csiszar (2013) data and stressed transition probability estimation results.

	k	AA1-2	AA3	A	BBB	BB	Default	$\mathbb{E}(\mathbf{I})$	$\bar{\theta}$
l_i		-3.20%	-1.07%	0.00%	3.75%	15.83%	51.80%		
p_i		0.09%	2.60%	90.75%	5.50%	1.00%	0.06%	0.37%	
\bar{p}_i (B&C)	2	0.036%	1.34%	53.53%	5.37%	4.91%	34.8%	19.07%	-
\bar{p}_i (MLT)	2	0.03%	1.33%	53.49%	5.38%	4.99%	34.78%	18.74%	13.49
\bar{p}_i (KL)	2	0.03%	1.33%	53.49%	5.38%	4.99%	34.78%	18.74%	13.49
\bar{p}_i (KL)	4	0.02%	0.73%	29.98%	3.28%	4.00%	62.00%	32.42%	15.76

	Aaa	Aa	A	Baa	Ba	B	Caa-C	D	KL
Aaa	-0.2101	0.2352	0.2485	0.0293	0.0000	0.0000	0.0000	0.0000	0.3029
Aa	0.0062	-0.2884	0.5494	0.1809	0.1114	0.0124	0.0000	0.0158	0.5876
A	0.0042	-0.0089	-0.2745	0.5777	0.2255	0.0309	0.0000	0.0204	0.5753
Baa	0.0000	0.0000	-0.0139	-0.2764	0.7209	0.2107	0.0000	0.0114	0.6527
Ba	0.0000	0.0000	0.0000	-0.0070	-0.2728	0.7228	0.0922	0.1085	0.6437
B	0.0000	0.0000	0.0000	0.0000	-0.0196	-0.2468	0.5773	0.2175	0.5284
Caa-C	0.0000	0.0000	0.0000	0.0161	0.0007	-0.0195	-0.0906	0.1538	0.0605
									3.3512

Scenarios are as defined in Vonatto (2012) with Kullback-Leibler relative entropy measured relative to Moody's average migration matrix (1921-2009).

Table 3. Annual Kullback-Leibler divergence estimates for Moody's and Fitch Global Corporate Ratings by ratings class, 2007-13.

Moody's (1920-2013 reference distribution)								
	max KL	2007	2008	2009	2010	2011	2012	2013
Aaa	$+\infty$	0.0160	0.0162	0.2862	0.0119	0.0140	0.1511	0.0268
Aa	7.19	0.0426	0.0423	0.1279	0.0130	0.1026	0.1977	0.0297
A	6.88	0.0760	0.0124	0.0615	0.0080	0.0384	0.0557	0.0261
Baa	5.83	0.0183	0.0121	0.0247	0.0393	0.0205	0.0335	0.0201
Ba	4.25	0.0193	0.0415	0.0475	0.0353	0.0294	0.0212	0.0118
B	3.22	0.0507	0.0686	0.0722	0.0414	0.0436	0.0469	0.0317
Caa	2.04	0.0566	0.0615	0.1370	0.0290	0.0421	0.0229	0.0381
Ca to C	1.23	0.1494	0.2630	1.0158	0.1509	0.2076	0.4229	0.5208
Total	-	0.4288	0.5177	1.7728	0.3288	0.4982	0.9520	0.7052

Moody's (1970-2013 reference distribution)								
	max KL	2007	2008	2009	2010	2011	2012	2013
Aaa	$+\infty$	0.0127	0.0808	0.2741	0.0082	0.0105	0.1416	0.0241
Aa	8.03	0.0686	0.0286	0.0565	0.0124	0.0449	0.1206	0.0558
A	7.37	0.0818	0.0095	0.0622	0.0071	0.0399	0.0572	0.0204
Baa	6.32	0.0167	0.0111	0.0264	0.0274	0.0147	0.0254	0.0121
Ba	4.45	0.0171	0.0376	0.0444	0.0312	0.0271	0.0184	0.0078
B	3.18	0.0514	0.0588	0.0606	0.0417	0.0413	0.0391	0.0279
Caa	1.93	0.0594	0.0594	0.1096	0.0315	0.0450	0.0256	0.0490
Ca to C	0.82	0.1690	0.0886	1.0158	0.0570	0.0874	0.1823	0.2475
Total	-	0.4767	0.3745	1.6495	0.2165	0.3108	0.6102	0.4446

Fitch (1990-2013 reference distribution)								
	max KL	2007	2008	2009	2010	2011	2012	2013
AAA	$+\infty$	0.0031	0.0396	0.2328	0.0028	0.0659	0.0659	0.0659
AA	7.82	0.0127	0.0712	0.1160	0.0059	0.1607	0.0492	0.0731
A	7.13	0.0220	0.0149	0.1203	0.0085	0.0253	0.0161	0.0057
BBB	6.21	0.0062	0.0069	0.0363	0.0249	0.0066	0.0132	0.0145
BB	4.42	0.0225	0.0270	0.0443	0.0300	0.0233	0.0224	0.0373
B	3.84	0.0415	0.0368	0.0862	0.0200	0.0176	0.0187	0.0234
CCC to C	1.32	0.1611	0.0797	0.3219	0.3403	0.0588	0.0140	0.1362
Total	-	0.2691	0.2762	0.9578	0.4324	0.3583	0.1996	0.3562

Table 4. DFAST domestic macroeconomic variables, descriptions, and data sources.¹

Macroeconomic Factor	Description	Data Source
<i>Economic Activity and Prices</i>		
Real Gross Domestic Product	Percent change in real GDP at an annualized rate	Bureau of Economic Analysis
Nominal Gross Domestic Product	Percent change in nominal GDP at an annualized rate	Bureau of Economic Analysis
Unemployment Rate	Quarterly average U.S. unemployment rate	Bureau of Labor Statistics
Real Disposable Income	Percent change in nominal disposable personal income divided by the price index for personal consumption expenditures at an annualized rate	Bureau of Economic Analysis
Nominal Disposable Income	Percent change in nominal disposable personal income at an annualized rate	Bureau of Economic Analysis
Consumer Price Index	Percent change in the CPI at an annualized rate	Bureau of Labor Statistics
<i>Asset Prices or Financial Conditions</i>		
House Prices	Seasonally adjusted index level	CoreLogic
Commercial Property Prices	Commercial Real Estate Price Index (series FI075035503.Q)	Federal Reserve Board
Equity Prices	End of quarter Dow Jones Stock Market Index	Dow Jones
U.S. Stock Market Volatility	VIX converted to quarterly	Chicago Board Options Exchange
<i>Interest Rates</i>		
3-month Treasury Bill	Quarterly average of 3-month Treasury bill secondary market rate discount basis	Federal Reserve Board
5-year Treasury Bond	Quarterly average of the yield on 5-year U.S. Treasury bonds	Federal Reserve Board ²
10-year Treasury Bond	Quarterly average of the yield on 10-year U.S. Treasury bonds	Federal Reserve Board ⁵

¹ Source: Board of Governors of the Federal Reserve System, “2015 Supervisory Scenarios for Annual Stress Tests Required under the Dodd-Frank Act Stress Testing Rules and the Capital Plan Rule,” October 23, 2014.

² Constructed for FRB/U.S. model by Federal Reserve staff based on the Svensson smoothed term structure model; see Lars E. O. Svensson (1995), “Estimating Forward Interest Rates with the Extended Nelson-Siegel Method,” Quarterly Review, no. 3, Sveriges Riksbank, pp. 13–26

10-year BBB Corporate Bond	Quarterly average of the yield on 10-year BBB-rated corporate bonds	Federal Reserve Board ³
Prime Rate	Quarterly average of monthly series	Federal Reserve Board
30-year Fixed Rate Mortgage	Quarterly average of 30-year fixed rates	Federal Home Loan Mortgage Corporation

³ Constructed for FRB/U.S. model by Federal Reserve staff using a Nelson-Siegel smoothed yield curve model; see Charles R. Nelson and Andrew F. Siegel (1987), "Parsimonious Modeling of Yield Curves," *Journal of Business*, vol. 60, pp. 473-89. Data prior to 1997 is based on the WARGA database. Data after 1997 is based on the Merrill Lynch database.

Table 5. Summary statistics for macroeconomic variables, Q1:1947 to Q2:2014.

<i>Statistics</i>	<i>GDP</i> ¹	<i>Unemployment</i> ²	<i>10-year Treasury</i> ³	<i>Dow Jones</i> ⁴
Minimum	-10.10%	2.60%	-4.63%	-26.52%
Maximum	16.58%	10.70%	13.38%	15.84%
Mean	3.24%	5.83%	2.44%	-1.76%
Standard Deviation	3.93%	1.66%	2.78%	6.77%
<i>2nd Moments and Cross Moments</i>				
	<i>GDP</i>	<i>Unemployment</i>	<i>10-year Treasury</i>	<i>Dow Jones</i>
<i>GDP</i>	0.002599			
<i>Unemployment</i>	0.001847	0.003688		
<i>10-year Treasury</i>	0.000845	0.001600	0.000774	
<i>Dow Jones</i>	0.000065	0.000133	0.000672	0.004890
<i>Correlation Matrix</i>				
	<i>GDP</i>	<i>Unemployment</i>	<i>10-year Treasury</i>	<i>Dow Jones</i>
<i>GDP</i>	1.0000			
<i>Unemployment</i>	-0.0912	1.0000		
<i>10-year Treasury</i>	0.0896	0.2273	1.0000	
<i>Dow Jones</i>	0.2390	0.1184	0.3499	1.0000

¹ Real rate of growth in gross domestic product² National rate of unemployment³ Real 10-year Treasury bond yield⁴ Real rate of growth in the Dow Jones Industrial Average

Table 6. Quarterly estimated Kullback-Leibler divergence ($D^{KL}(\mathbf{p}^* \parallel \mathbf{q}^*)$) for each DFAST scenario.

Quarter	$D^{KL}(\mathbf{p} \parallel \mathbf{q}^*)$		
	Base	Adverse	Severe
2014 Q4	0.0662	0.7773	7.0512
2015 Q1	0.0742	0.9949	8.3588
2015 Q2	0.0661	0.9357	6.8611
2015 Q3	0.0609	0.9743	4.7658
2015 Q4	0.0607	1.0163	2.7851
2016 Q1	0.0533	0.8797	2.7359
2016 Q2	0.0530	0.7394	2.7637
2016 Q3	0.0530	0.6582	3.1003
2016 Q4	0.0527	0.6573	3.2228
2017 Q1	0.0475	0.6185	3.2575
2017 Q2	0.0437	0.5710	2.4104
2017 Q3	0.0478	0.5237	2.2626
2017 Q4	0.0439	0.4675	1.6439

Table 7. Estimated Lagrange multipliers (shadow prices) on moment consistency equations by DFAST scenario and quarter.

Quarter	Base				Adverse				Severe			
	<i>GDP</i>	<i>UNEM</i>	<i>10YTY</i>	<i>DJIA</i>	<i>GDP</i>	<i>UNEM</i>	<i>10YTY</i>	<i>DJIA</i>	<i>GDP</i>	<i>UNEM</i>	<i>10YTY</i>	<i>DJIA</i>
Q3: 2014	-1.14	-0.54	10.29	-1.30	15.73	-10.46	13.16	12.29	34.06	-19.55	261.80	54.15
Q4:2014	-0.69	1.55	11.23	-0.86	19.28	-20.09	14.16	12.36	55.67	-42.55	55.91	80.79
Q1:2015	-0.68	3.69	10.33	-0.80	13.76	-25.99	16.15	12.73	33.98	-67.75	27.42	63.66
Q2:2015	-0.68	5.87	9.44	-0.68	11.82	-30.04	18.21	12.73	29.74	-116.77	21.41	30.63
Q3:2015	-0.69	10.46	7.67	-0.75	11.34	-34.27	15.18	13.29	20.34	-767.86	17.07	3.52
Q4:2015	-0.68	10.46	6.81	-0.66	8.98	-38.72	13.28	11.22	7.12	-727.08	22.62	-10.54
Q1:2016	-0.67	10.46	6.82	-0.55	7.11	-41.05	11.42	8.86	7.12	-690.95	25.03	-10.11
Q2:2016	-0.69	12.87	5.13	-0.56	4.80	-41.05	9.64	8.16	-1.14	-737.37	23.80	-18.10
Q3:2016	-0.69	12.88	5.15	-0.38	4.34	-43.47	7.90	7.63	-1.14	-786.76	21.45	-20.97
Q4:2016	0.22	12.87	4.32	-0.34	4.34	-43.47	7.05	6.79	-5.24	-155.41	20.31	-28.78
Q1:2017	0.22	12.87	3.50	-0.33	3.88	-43.48	4.56	5.99	-5.23	-117.03	17.09	-19.39
Q2:2017	0.68	12.87	4.33	-0.12	3.42	-43.47	2.93	4.68	-5.23	-96.61	15.04	-21.04
Q3:2017	0.68	12.87	3.51	-0.12	2.51	-43.48	1.31	2.03	-5.24	-82.90	14.06	-13.47

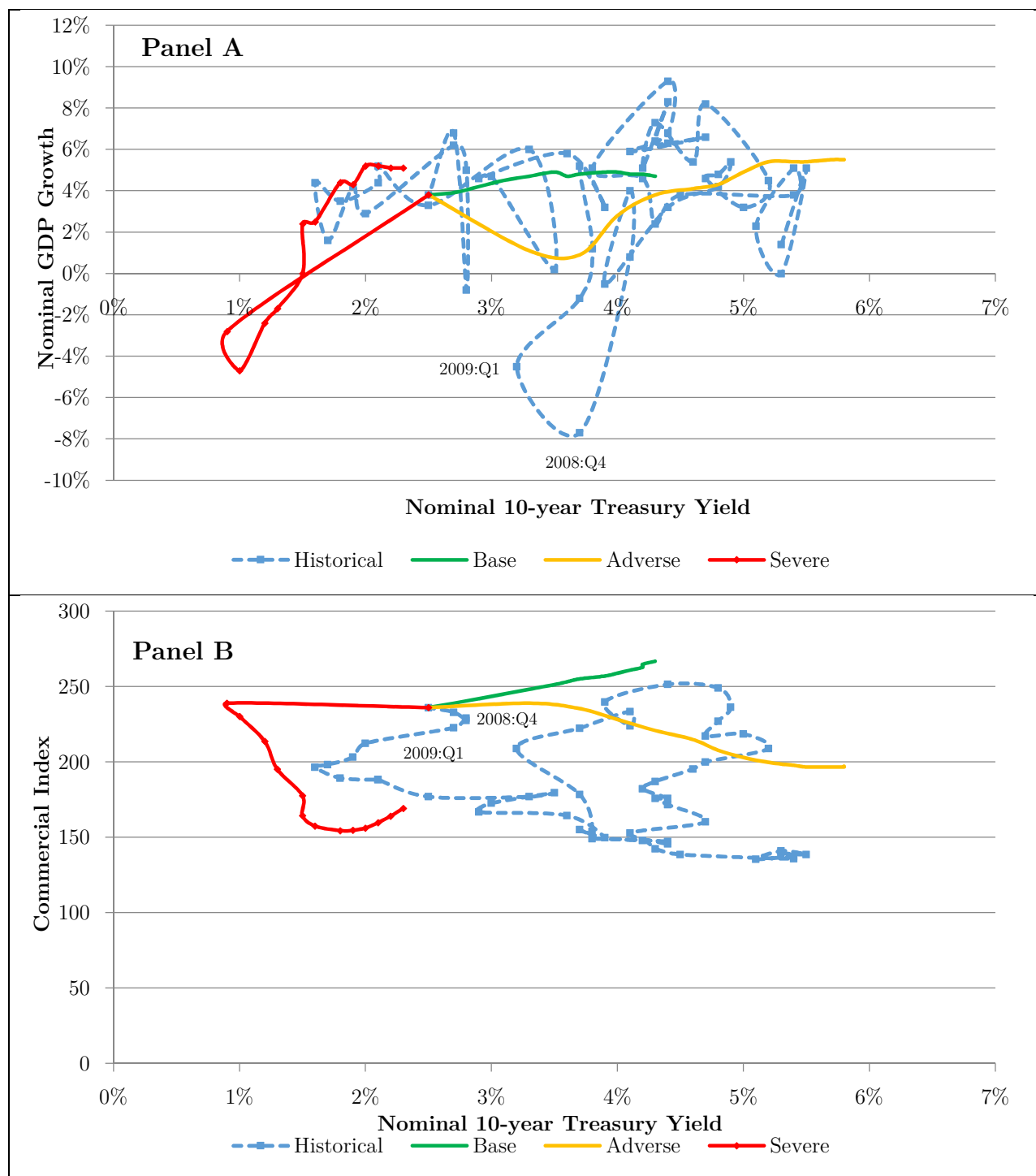


Figure 1. Phase graphs for DFAST macroeconomic variable data as released (2001:Q1 to 2017:Q4) for nominal 10-year treasury yield vs. nominal GDP growth (panel 1) and nominal 10-year treasury yield vs. commercial real estate index (panel 2).

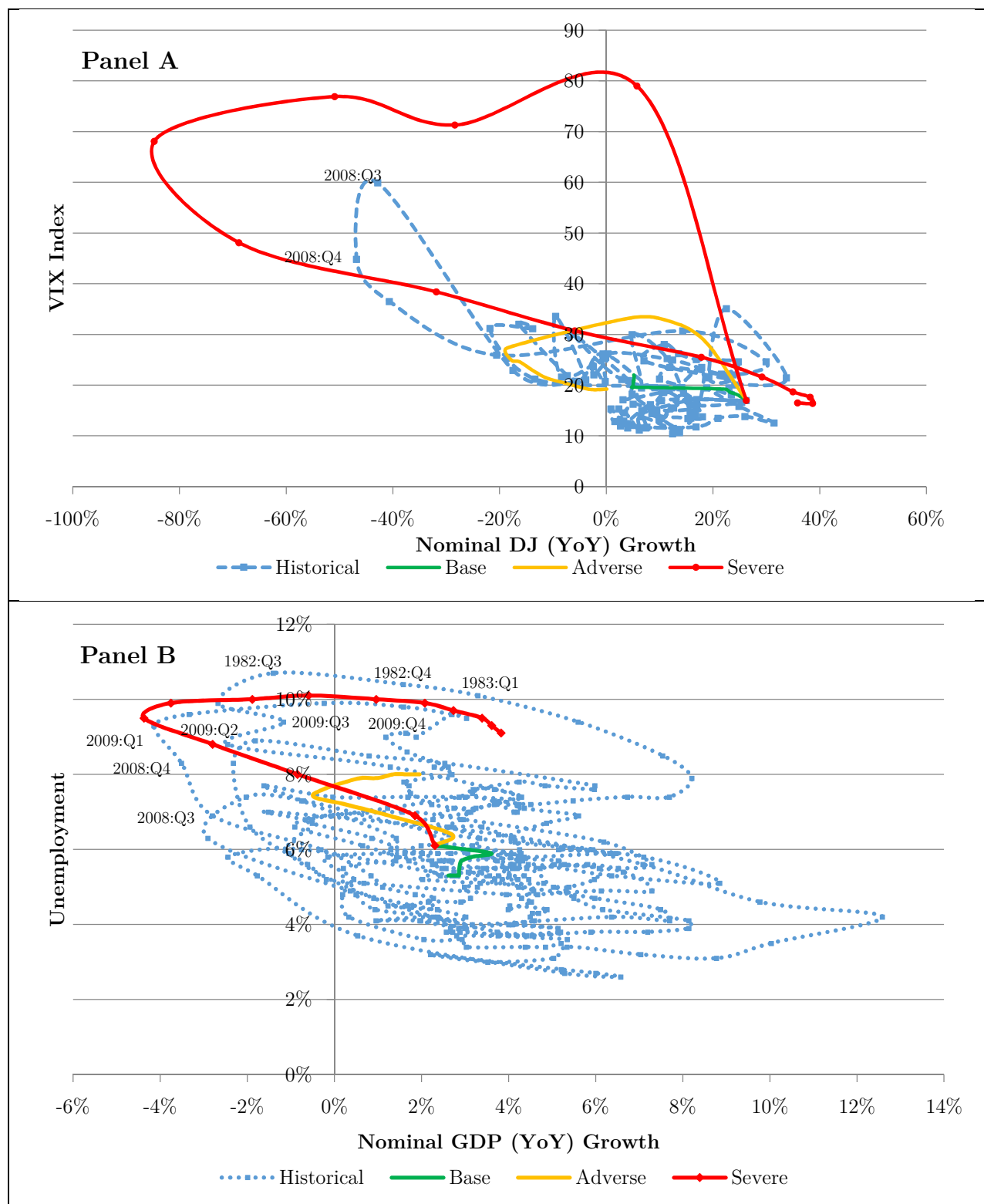


Figure 2. Phase graphs for DFAST macroeconomic variables: unemployment and VIX as released and constructed DJ and GDP year-over-year growth. Data are from 1990:Q1 for nominal Dow Jones Stock Index year-over-year growth vs. VIX Index (panel 1) and 1948:Q1 for nominal GDP year-over-year growth vs. unemployment (panel 2).

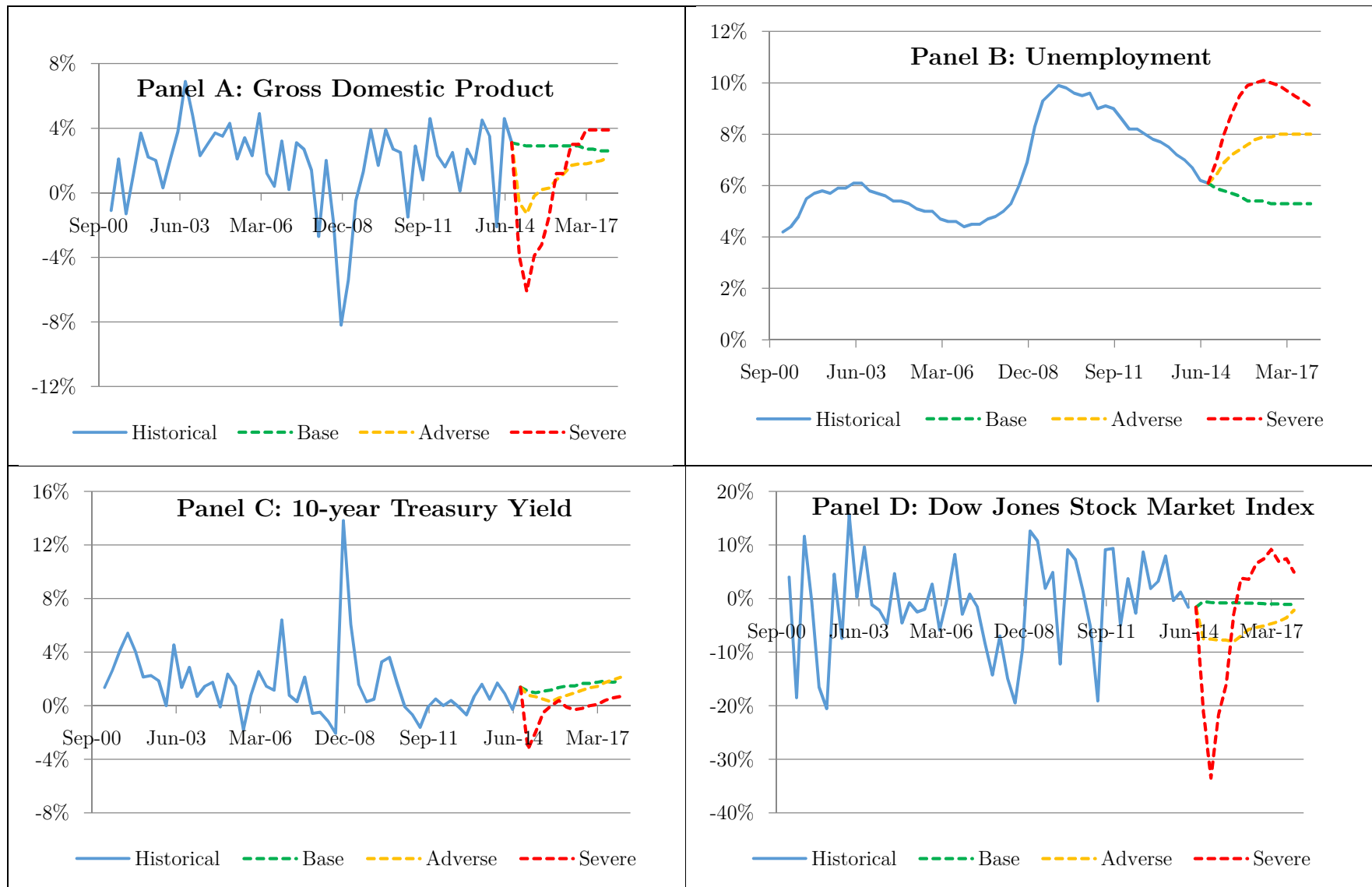


Figure 3. Historical and DFAST scenarios for real GDP growth (panel 1), unemployment rate (panel 2), real 10-year treasury yield (panel 3), and real rate of growth in the Dow Jones Stock Market Index (panel 4).

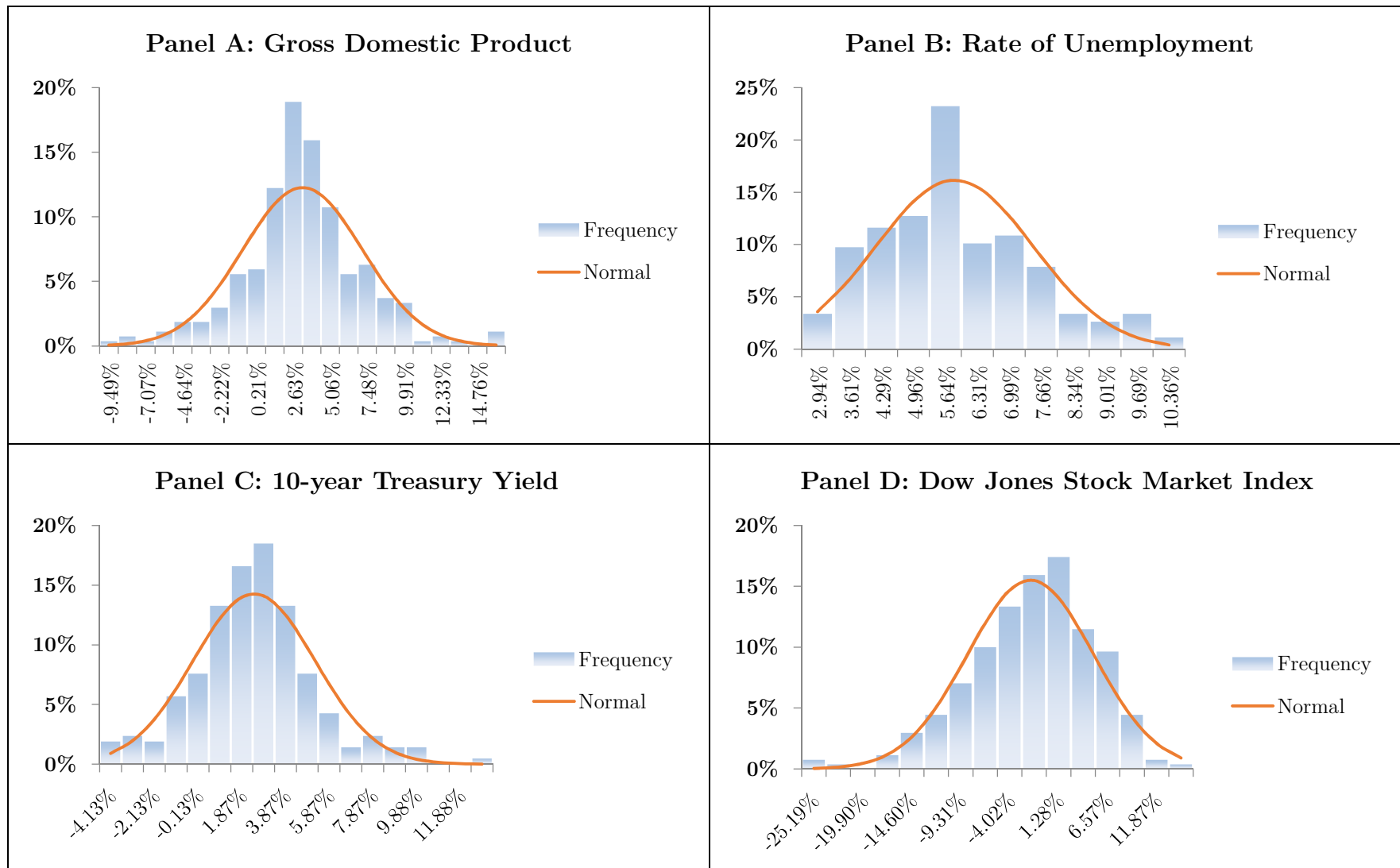


Figure 4. Estimated histograms for real GDP growth (panel 1), unemployment rate (panel 2), real 10-year treasury yield (panel 3), and real rate of growth in the Dow Jones Industrial Average (panel 4) from quarterly data, Q1:1947 to Q2:2013.

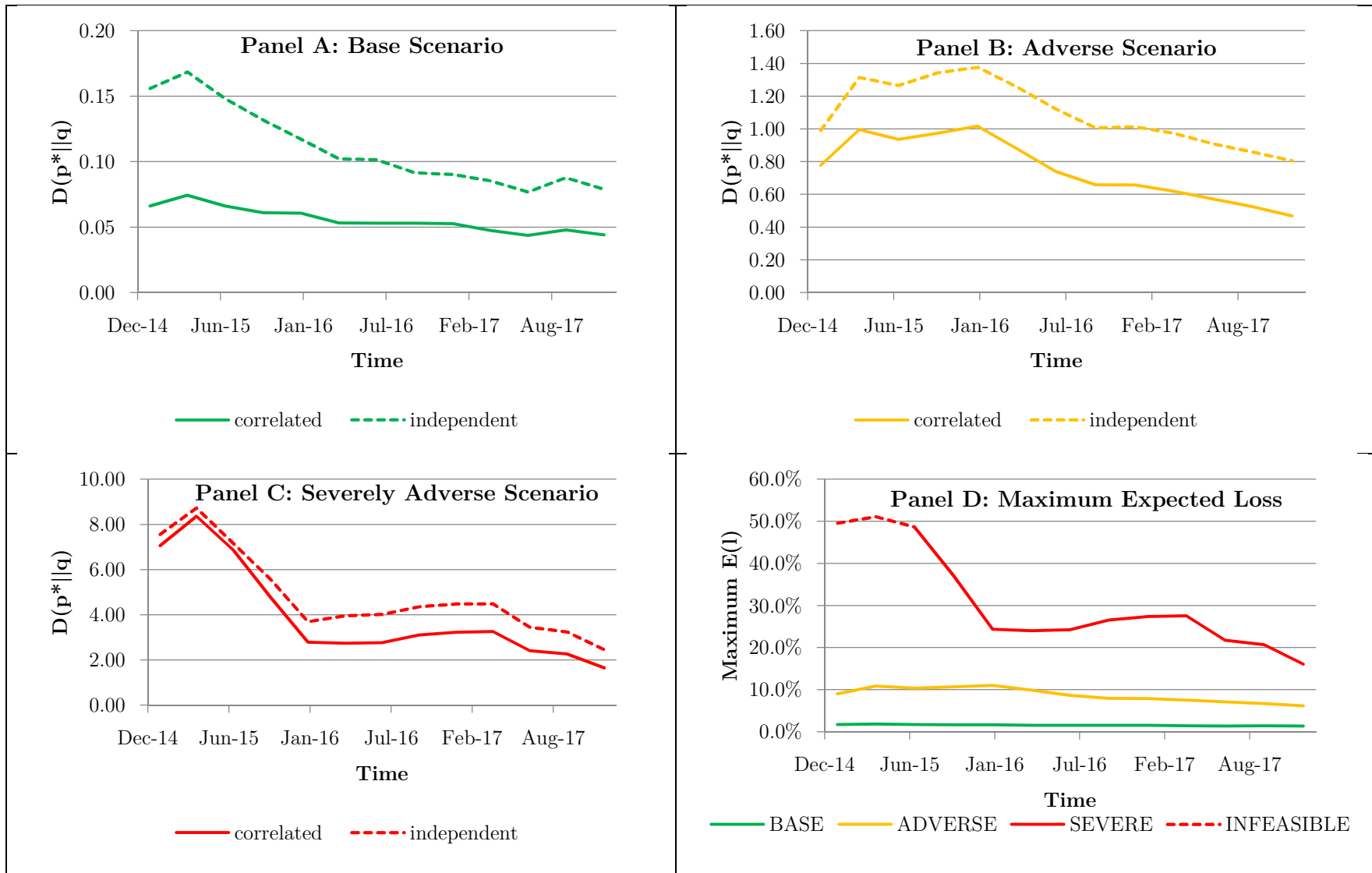


Figure 5. Panels 1-3: estimated quarterly KL Divergence for base, adverse and severely adverse DFAST scenarios assuming independent and correlated macroeconomic factors. Panel 4: expected (maximum) credit losses implied by each DFAST scenario.

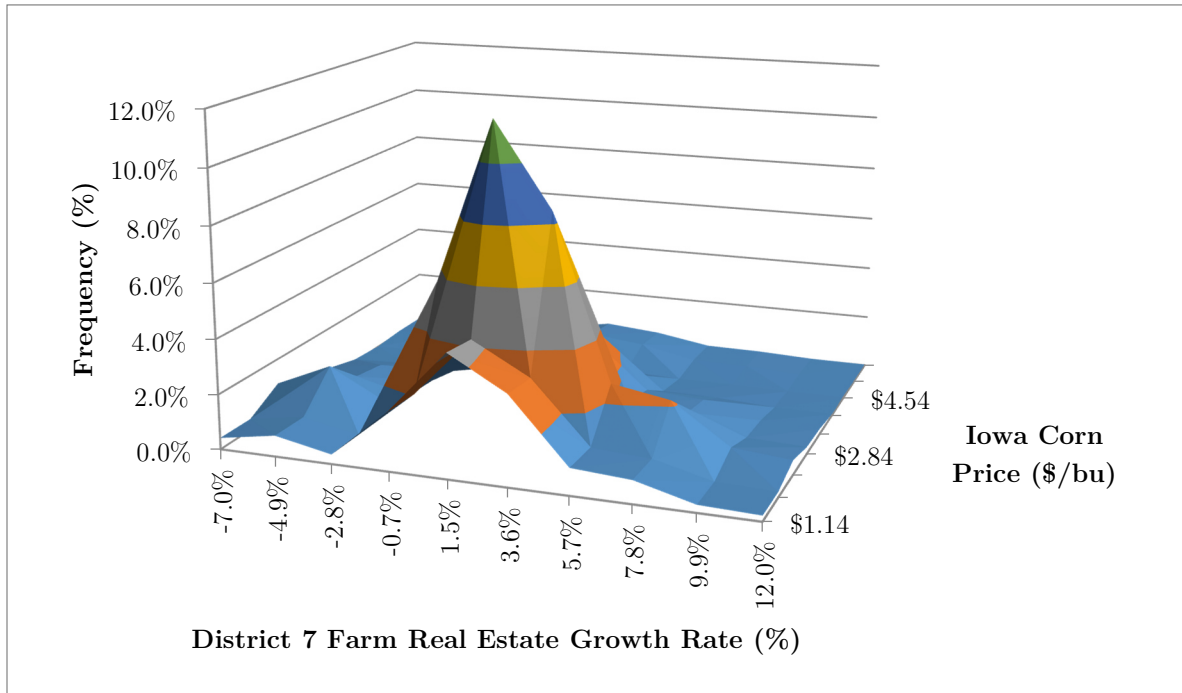


Figure 6. Empirical frequency distribution for the rate of growth in 7th district farm real estate values and the price per bushel of corn in Iowa assuming independence.

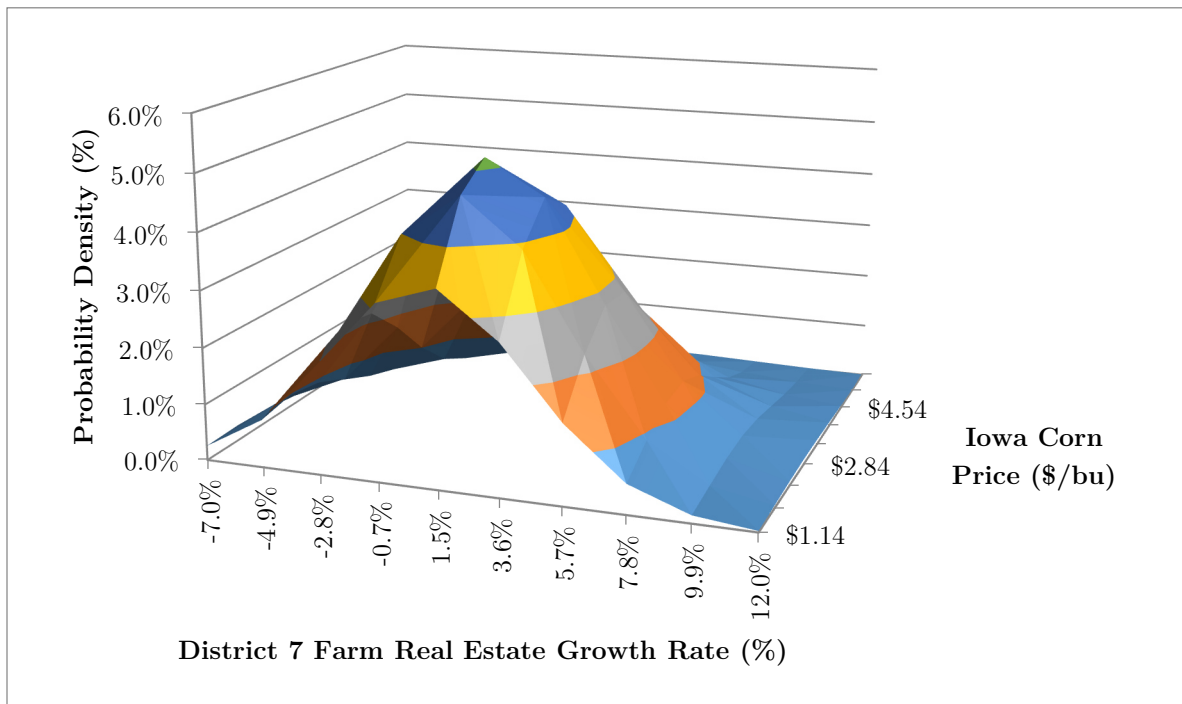


Figure 7. Estimated joint density for the rate of growth in 7th district farm real estate values and the price per bushel of corn in Iowa assuming empirical correlation equal to 0.1833.

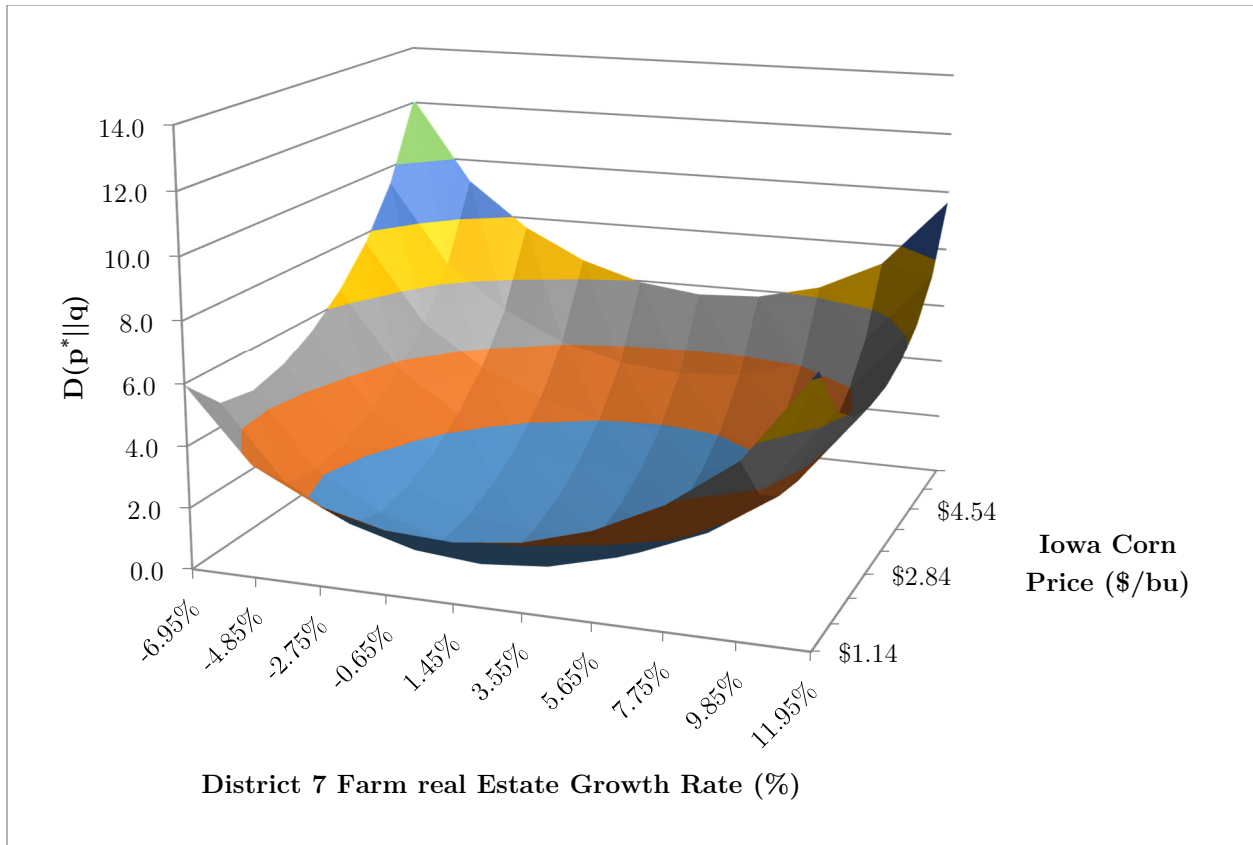


Figure 8. Estimated Kullback-Leibler relative entropy between the rate of growth in 7th district farmland value and the price per bushel of corn in Iowa.